Spectrum and energy levels of five-times ionized zirconium (Zr VI)

2016 Phys. Scr. 91 025401

(http://iopscience.iop.org/1402-4896/91/2/025401)

IOP Publishing | Royal Swedish Academy of Sciences Physica Scripta

Phys. Scr. **91** (2016) 025401 (22pp) doi:10.1088/0031-8949/91/2/025401

Spectrum and energy levels of five-times ionized zirconium (Zr VI)

Joseph Reader and Mark D Lindsay

National Institute of Standards and Technology, Gaithersburg, MD 20899-8422, USA

E-mail: joseph.reader@nist.gov

Received 19 August 2015, revised 4 November 2015
Accepted for publication 2 December 2015
Published 5 January 2016

Abstract

We carried out a new analysis of the spectrum of five-times-ionized zirconium Zr VI. For this we used sliding-spark discharges together with normal- and grazing-incidence spectrographs to observe the spectrum from 160 to 2000 Å. These observations showed that the analysis of this spectrum by Khan *et al* (1985 *Phys. Scr.* **31** 837) contained a significant number of incorrect energy levels. We have now classified ~420 lines as transitions between 23 even-parity levels 73 odd-parity levels. The $4s^24p^5$, $4s4p^6$, $4s^24p^44d$, 5s, 5d, 6s configurations are now complete, although a few levels of $4s^24p^45d$ are tentative. We determined Ritz-type wavelengths for ~135 lines from the optimized energy levels. The uncertainties range from 0.0003 to 0.0020 Å. Hartree–Fock calculations and least-squares fits of the energy parameters to the observed levels were used to interpret the observed configurations. Oscillator strengths for all classified lines were calculated with the fitted parameters. The results are compared with values for the level energies, percentage compositions, and transition probabilities from recent *ab initio* theoretical calculations. The ionization energy was revised to 777 380 ± 300 cm^{-1} (96.38 ± 0.04 eV).

Keywords: zirconium, spectrum, energy levels, wavelengths, ionization energy, transition probabilities, ultraviolet

(Some figures may appear in colour only in the online journal)

1. Introduction

The zirconium atom has atomic number $Z = 40$. Five-times-ionized zirconium, Zr VI, is isoelectronic with neutral Br. The ground state is $4s^24p^5\ ^2P$, and excited states are mainly of the type $4s^24p^4nl$. The first work on this spectrum was done by Paul and Rense [1]. From their observation of transitions to the ground term, they determined the $4p^5\ ^2P$ interval as well as the first excited state $4s4p^6\ ^2S_{1/2}$ and several levels of the $4p^44d$ and $4p^45s$ configurations. Subsequently, Chaghtai [2, 3] re-observed the resonance transitions and found that nearly all of Paul and Rense's excited levels were in error. Chaghtai gave values for 16 new levels in these configurations. Subsequently, Ekberg *et al* [4] re-investigated the spectrum and gave improved values for nearly all levels of the $4p^44d$ and 5s configurations. Seven of Chaghtai's levels were found to be spurious. Chaghtai *et al* [5] later extended the resonance lines to the $4p^45d$, 6s, 6d, and 7s configurations. Khan *et al* [6] determined the levels of the $4p^45p$ configuration by using longer wavelength transitions from the above configurations to levels of $4p^45p$.

In the present work we re-observed the spectrum of Zr VI in the vacuum ultraviolet and revised the analysis considerably. In particular, 13 of the 21 levels of $4p^45p$ reported by Khan *et al* [6] were found to be spurious. Several new levels of $4p^44d$, 5s, 5d, and 6s reported in [6] were also found to be spurious.

2. Experiment

The observations used for this work were the same as used for earlier work in our laboratory on zirconium [7]. The main light source was a low-voltage sliding-spark with metallic Zr electrodes. The source was operated as described by Reader *et al* [8]. From 500 to 2000 Å the spectra were recorded on our 10.7 m normal-incidence vacuum spectrograph. From 160 to 500 Å the spectra were recorded on our 10.7 m grazing incidence spectrograph. Both instruments had gratings with 1200 lines/mm. The plate factor for the normal-incidence spectrograph was about 0.78 Å mm^{-1}. The plate factor for the grazing-incidence spectrograph at 350 Å was 0.25 Å mm^{-1}. From 600 to 2000 Å the spectra were calibrated by spectra of Cu II excited in a hollow cathode discharge. Below 600 Å calibration was obtained from lines of Y in various stages of ionization. Shifts between the positions of the reference spectra and those of the unknown spectra due to differing illumination of the spectrograph were removed by use of impurity lines of oxygen, nitrogen, carbon, and silicon. Complete references for the calibration spectra are given in [7].

Ionization stages were distinguished by comparing the intensities of the lines at various peak currents in the spark. The spectra of Zr VI were relatively enhanced at a peak current of about 2000 A.

The wavelengths, intensities, and classifications of the observed lines of Zr VI are given in table 1. The intensities are estimates of photographic plate blackening. No effort was made to harmonize the intensities through the complete region of observation. The general uncertainty of the wavelengths is ±0.005 Å. Hazy lines (h) were given an uncertainty of ±0.010 Å; perturbed (p), or asymmetric lines (s, l) an uncertainty of ±0.020; unresolved (u) or doubly classified (dc) lines an uncertainty of ±0.030 Å. By *perturbed* we mean that the measured position may possibly be affected by the presence of a close line. The line at 1749.353 Å could not be measured in the original observations because of a local defect in the emulsion of one of the photographic plates. It was later recorded with an image plate [9, 10] on the normal-incidence spectrograph. Its wavelength uncertainty was also taken as ±0.005 Å. All uncertainties are reported at the level of one standard deviation.

3. Spectrum analysis and level value determination

The analysis was carried out in a manner similar to that used for the recent analysis of Mo V [11]. As described there 'Interpretation of the spectrum was guided by calculations of the level structures and transition probabilities with the Hartree–Fock code of Cowan [12]. Further guidance was provided by construction of two-dimensional transition arrays with the computer spreadsheet method described by Reader [13]'.

The odd parity energy levels are given in table 2, the even levels in table 3. In addition to the usual spectroscopic designations in either LS or *jl* (pair) coupling, the levels are given shorthand designations that are used in the classification of the spectral lines. The shorthand designations are explained in the footnotes to tables 2 and 3. As described in [11] 'the values of the energy levels were optimized with the computer program ELCALC [14], an iterative procedure in which the observed wave numbers are weighted according to the inverse square of their uncertainties. The uncertainties of the level values given by this procedure are also listed'. For the level optimization only the most reliably classified lines were used. That is, lines that were very weak or that appeared with suspiciously high intensities were excluded.

Figure 1 shows a schematic overview of the positions of the $4s^24p^5$, $4s4p^6$, $4s^24p^44d$, 5s, 5p, 5d, and 6s, configurations. It also shows the calculated positions of the $4s^24p^44f$ and $4s4p^54d$ configurations, although no levels have as yet been established for them.

3.1. $4s^24p^44d$ levels

Nearly all levels of this configuration that could combine with the ground state were present in [4]. Remaining as unknown were $(^3P)^4D_{1/2,7/2}$, $(^1S)^2D_{5/2}$, $(^3P)^4F_{7/2/9/2}$, $(^3P)^2F_{7/2}$, $(^1D)^2G_{7/2,9/2}$, and $(^1D)^2F_{7/2}$. Values for these 9 levels were given in [6]. Our present work shows that 6 of the 9 were spurious. Details of these 9 levels are:

(1) $(^3P)^4D_{1/2}$—new level; two new resonance lines (397.112 and 423.344 Å) and three transitions to levels of $4p^45p$
(2) $(^3P)^4D_{7/2}$—new level; four strong transitions to levels of $4p^45p$
(3) $(^1S)^2D_{5/2}$—new level; one new resonance line (307.148 Å) and three transitions to levels of $4p^45p$
(4) $(^3P)^4F_{7/2}$—present in [6]; five transitions to levels of $4p^45p$
(5) $(^3P)^4F_{9/2}$—new level; single line at 602.387 Å, places $(^3P)^4F_{9/2}$ close to prediction
(6) $(^3P)^2F_{7/2}$—new level; six transitions to levels of $4p^45p$
(7) $(^1D)^2G_{7/2}$—new level; four transitions to levels of $4p^45p$
(8) $(^1D)^2G_{9/2}$—present in [6]; single line at 600.282 Å; places $(^1D)^2G_{9/2}$ close to prediction
(9) $(^1D)^2F_{7/2}$—present in [6]; six transitions to levels of $4p^45p$.

We note that the two $J = 9/2$ levels of $4p^44d$ are established by single transitions that are close in wavelength, 600.282 Å and 602.387 Å. Thus, one could consider interchanging their classifications without changing the level values very much. Our present classifications were chosen to provide the best match with the level values given by the least-squares fit (LSF) with the Cowan code, described in section 4 below.

The structure of the $4p^44d$ configuration is shown in figure 2. This is similar to figure 1 of [4], except that we show here the observed positions of levels that were previously unknown.

3.2. $4s^24p^45s$ levels

The $4s^24p^45s$ levels [1, 2, 4] have improved values due to their combinations with $4s^24p^45p$. For completeness, in figure 3 we give the structure of the $4p^45s$ configuration. This is the same as figure 2 of [4], except that here we designate the levels in *jl* coupling, rather than J_1j. This coupling scheme is more now more commonly used for np^4ns configurations.

Table 1. Observed spectral lines of Zr VI. Wavelengths and wave numbers are in vacuum. Wavelength values in parentheses are Ritz values. General uncertainty of the observed wavelengths is ±0.005 Å. Uncertainties for less certain wavelengths are given in section 2 of text. Acc. is the accuracy estimate.

λ_{obs}(Å)	Intensity		σ_{obs}(cm^{-1})	Even level[a]	Odd level[a]	λ_{Ritz}(Å)	Unc(λ_{Ritz}-Å)	$g_U A$(s^{-1})	log $(g_L f)$	|CF|	Acc.
165.930	5		602 664	6s31	p5 3	165.9308	0.0011	2.28E + 09	−2.03	0.15	D+
170.342	6		587 054	6s31	p5 1	170.3408	0.0012	6.37E + 09	−1.56	0.60	D+
174.066	6		574 495	5d85	p5 3	174.0660	0.0003	2.46E + 09	1.95	0.30	D+
174.489	70		573 102	6s25	p5 3	174.4891	0.0003	2.27E + 10	0.99	0.65	D+
178.236	50		561 054	6s21	p5 3	178.2371	0.0003	9.00E + 09	1.37	0.54	D+
178.776	60		559 359	6s23	p5 3	178.7769	0.0003	8.48E + 09	1.39	0.55	D+
178.794	30		559 303	5d83	p5 1	178.7993	0.0004	6.19E + 09	1.53	0.26	D+
179.144	10		558 210	6s11	p5 3	179.1445	0.0003	1.17E + 09	2.25	0.51	E
179.308	70		557 700	6s33	p5 1	179.3084	0.0003	2.14E + 10	0.99	0.70	D+
182.213	30		548 808	5d73	p5 3	182.2139	0.0003	3.07E + 09	1.82	0.16	D+
182.550	20		547 795	5d51	p5 3			4.24E + 09	1.67	0.14	D+
182.657	90		547 474	6s13	p5 3	182.6578	0.0003	1.86E + 10	1.03	0.25	D+
182.744	80		547 214	5d75	p5 3	182.7439	0.0003	1.34E + 10	1.18	0.45	D+
183.262	70		545 667	5d65	p5 3	183.2623	0.0003	9.69E + 09	1.31	0.35	D+
183.336	60	dc	545 447	6s15	p5 3	183.3357	0.0004	2.33E + 09	1.93	0.67	D+
183.336	60	dc	545 447	6s21	p5 1	183.3471	0.0003	1.07E + 10	1.27	0.40	D+
183.680	90		544 425	5d63	p5 3			3.65E + 10	0.73	0.50	D+
183.908	5		543 750	6s23	p5 1	183.9068	0.0004	1.19E + 09	2.22	0.35	E
184.063	60		543 292	5d41	p5 3	184.0618	0.0003	6.50E + 09	1.48	0.17	D+
187.075	20		534 545	5d53	p5 3	187.0723	0.0003	2.64E + 09	1.86	0.06	D+
187.361	100		533 729	5d55	p5 3	187.3582	0.0003	2.74E + 10	0.84	0.41	D+
187.549	80		533 194	5d73	p5 1	187.5459	0.0004	2.50E + 10	0.88	0.42	D+
187.830	5	ℓ	532 396	5d45	p5 3	187.8277	0.0003	1.04E + 09	2.26	0.25	E
187.905	60		532 184	5d51	p5 1			1.67E + 10	1.05	0.44	D+
188.490	20		530 532	5d43	p5 3	188.4876	0.0003	2.23E + 09	1.93	0.20	D+
188.912	2	x	529 347	5d35	p5 3	188.9103	0.0003	1.89E + 08	3.00	0.05	E
189.046	3		528 972	5d33	p5 3	189.0444	0.0003	7.85E + 08	2.38	0.31	E
189.101	30		528 818	5d63	p5 1			6.39E + 09	1.47	0.29	D+
189.267	2		528 354	5d31	p5 3	189.2658	0.0003	3.84E + 08	2.69	0.11	E
189.506	5		527 688	5d41	p5 1	189.5041	0.0004	4.92E + 08	2.58	0.02	E
191.557	90		522 038	5d25	p5 3	191.5577	0.0003	2.73E + 10	0.82	0.43	D+
191.666	80		521 741	5d23	p5 3	191.6663	0.0004	1.43E + 10	1.10	0.42	D+
192.182	20	u, J	520 340	5d21	p5 3	192.1679	0.0004	2.51E + 09	1.86	0.20	D+
192.696	60		518 952	5d53	p5 1	192.6968	0.0004	7.84E + 09	1.36	0.23	D+
194.108	1		515 177	5d13	p5 3	194.1104	0.0003	5.39E + 07	3.52	0.01	E
194.197	20	p, x	514 941	5d43	p5 1	194.1988	0.0004	2.32E + 09	1.88	0.12	D+
195.024	2	x	512 757	5d31	p5 1	195.0250	0.0004	4.35E + 08	2.61	0.08	E
197.575	80		506 137	5d23	p5 1	197.5749	0.0005	1.90E + 09	1.95	0.05	D+
236.281	100		423 225	5s31	p5 3	236.2818	0.0005	3.14E + 09	1.58	0.06	D+
245.327	90	u	407 619	5s31	p5 1	245.3261	0.0006	1.62E + 10	0.84	0.47	D+
253.678	80		394 201	5s33	p5 3	253.6812	0.0005	2.26E + 09	1.66	0.04	D+
254.092	400		393 558	5s25	p5 3	254.0939	0.0005	6.20E + 10	0.22	0.65	C
259.888	200		384 781	5s21	p5 3	259.8878	0.0006	2.91E + 10	0.53	0.67	D+
263.310	500		379 780	5s23	p5 3	263.3127	0.0006	4.96E + 10	0.29	0.83	C
264.142	90	p	378 584	5s33	p5 1	264.1361	0.0007	4.67E + 10	0.31	0.61	C
264.940	100		377 444	5s11	p5 3	264.9343	0.0006	6.57E + 08	2.16	0.15	D+
270.480	200		369 713	5s13	p5 3	270.4811	0.0006	6.60E + 10	0.14	0.74	C
270.872	200		369 178	5s21	p5 1	270.8716	0.0007	3.75E + 10	0.39	0.61	C
274.105	200		364 824	5s15	p5 3	274.1024	0.0006	2.76E + 09	1.51	0.33	D+
274.598	100		364 169	5s23	p5 1	274.5941	0.0007	4.14E + 09	1.33	0.24	D+
276.364	80		361 842	5s11	p5 1	276.3582	0.0007	2.53E + 07	3.54	0.01	E
279.198	90	p	358 169	4d83	p5 3	279.1985	0.0007	1.78E + 10	0.68	0.05	D+
282.400	90		354 108	5s13	p5 1	282.3990	0.0008	3.56E + 09	1.37	0.10	D+
288.730	200		346 344	4d51	p5 3	288.7290	0.0008	2.75E + 10	0.46	0.11	D+
290.949	500		343 703	4d85	p5 3	290.9433	0.0007	1.05E + 12	1.12	0.85	C
291.920	500	p	342 560	4d83	p5 1	291.9151	0.0009	6.60E + 11	0.93	0.85	C

Table 1. (Continued.)

$\lambda_{\rm obs}$(Å)	Intensity		$\sigma_{\rm obs}$(cm^{-1})	Even level[a]	Odd level[a]	$\lambda_{\rm Ritz}$(Å)	Unc($\lambda_{\rm Ritz}$-Å)	$g_U A$(s^{-1})	log $(g_L f)$	|CF|	Acc.
294.395	500		339 680	4d73	p5 3	294.3923	0.0007	5.84E + 11	0.88	0.90	C
298.779	300		334 696	4d41	p5 3	298.7796	0.0008	2.81E + 11	0.58	0.71	C
302.351	300		330 741.4	4d51	p5 1	302.3498	0.0010	2.56E + 11	0.55	0.87	C
307.148	30		325 575.9	4d75	p5 3	307.1472	0.0010	3.16E + 06	4.35	0.00	E
308.569	100		324 076.6	4d73	p5 1	308.5658	0.0009	4.65E + 09	1.18	0.02	D+
313.150	300		319 335.8	4d63	p5 3	313.1496	0.0010	1.27E + 10	0.73	0.11	D+
313.389	300		319 092.2	4d41	p5 1	313.3891	0.0010	2.55E + 10	0.43	0.11	C
329.242	300		303 728.0	4d63	p5 1	329.2361	0.0012	1.31E + 10	0.67	0.06	D+
333.768	400		299 609.3	4d65	p5 3	333.7687	0.0010	2.97E + 09	1.31	0.10	D+
340.915	30		293 328.2	4p61	5p83	340.9169	0.0011	1.38E + 09	1.62	0.02	E
343.493	10		291 126.7	4p61	5p61	343.4908	0.0011	2.34E + 07	3.38	0.02	E
348.262	200	p	287 140.1	4d55	p5 3	348.2592	0.0012	9.38E + 08	1.77	0.01	D+
353.221	250		283 108.9	4d45	p5 3	353.2171	0.0011	2.40E + 09	1.35	0.01	D+
357.837	30		279 456.8	4d53	p5 3	357.8365	0.0012	2.21E + 08	2.37	0.00	D+
358.755	300		278 741.8	4d35	p5 3	358.7544	0.0012	1.71E + 09	1.48	0.02	D+
364.080	300		274 664.9	4d43	p5 3	364.0791	0.0013	1.52E + 09	1.52	0.01	D+
366.095	60	p	273 153.1	4p61	5p51	366.0947	0.0012	9.72E + 08	1.71	0.18	D+
366.522	200		272 834.9	4d33	p5 3	366.5226	0.0014	2.11E + 09	1.37	0.02	D+
367.523	300		272 091.8	4d31	p5 3	367.5238	0.0015	1.72E + 09	1.46	0.15	D+
368.494	300		271 374.8	4d25	p5 3	368.4947	0.0015	1.28E + 09	1.58	0.61	D+
368.600	250		271 296.8	4d23	p5 3	368.6010	0.0013	8.52E + 08	1.76	0.01	D+
375.546	30		266 279.0	4d21	p5 3	375.5467	0.0015	2.99E + 07	3.20	0.00	E
378.342	60		264 311.1	4p61	5p63	378.3472	0.0013	1.61E + 09	1.46	0.27	D+
378.992	80		263 857.8	4d53	p5 1	378.9969	0.0015	6.03E + 07	2.89	0.00	E
386.007	250		259 062.7	4d43	p5 1	386.0068	0.0016	1.55E + 09	1.46	0.01	D+
388.754	20		257 232.1	4d33	p5 1	388.7546	0.0018	3.39E + 07	3.12	0.00	E
389.881	100	p	256 488.5	4d31	p5 1	389.8811	0.0019	1.43E + 08	2.49	0.01	E
391.094	100	p	255 693.0	4d23	p5 1	391.0936	0.0017	3.67E + 07	3.07	0.00	E
397.112	30		251 818.1	4d11	p5 3			2.79E + 07	3.18	0.01	E
398.588	2		250 885.6	4p61	5p43	398.5922	0.0014	2.20E + 08	2.28	0.15	D+
398.919	80		250 677.5	4d21	p5 1	398.9218	0.0019	1.53E + 08	2.44	0.00	E
399.967	80		250 020.6	4d13	p5 3	399.9718	0.0018	4.90E + 07	2.93	0.00	E
401.701	80		248 941.4	4d15	p5 3	401.7031	0.0019	5.69E + 07	2.86	0.00	E
411.136	4		243 228.5	4p61	5p21	411.1384	0.0016	7.96E + 07	2.70	0.08	E
423.344	5		236 214.5	4d11	p5 1			1.93E + 07	3.29	0.00	E
514.611	1	x	194 321.5	4d13	5p41			2.32E + 08	2.04	0.07	D+
516.763	10		193 512.3	4d15	5p43			7.64E + 08	1.52	0.06	D+
516.970	10	x	193 434.8	4d27	5p55	516.9686	0.0014	3.09E + 08	1.91	0.06	E
522.000	2000		191 570.9	4p61	p5 3			2.62E + 09	0.97	0.04	D+
522.929	20		191 230.5	4d17	5p35			1.95E + 09	1.10	0.08	D+
524.835	5		190 536.1	4d13	5p35			2.97E + 08	1.91	0.06	D+
530.404	5	x	188 535.5	4d15	5p33			1.43E + 08	2.22	0.01	D+
532.528	10	s	187 783.6	4d23	5p73	532.5335	0.0017	6.94E + 08	1.53	0.11	D+
533.450	30		187 459.0	4d13	5p33			7.08E + 08	1.52	0.10	D+
535.216	80		186 840.5	4d13	5p31			1.16E + 09	1.30	0.12	D+
538.618	5		185 660.3	4d11	5p33			3.24E + 08	1.85	0.12	D+
539.350	70	ℓ, x	185 408.4	4d13	5p23			3.38E + 07	2.83	0.00	E
539.765	10	ℓ, x	185 265.8	4d53	5p51	539.7620	0.0014	1.46E + 08	2.20	0.02	D+
540.791	40		184 914.3	4d43	5p55	540.7885	0.0015	1.06E + 09	1.33	0.24	E
541.756	10	x	184 584.9	4d23	5p63	541.7643	0.0017	1.56E + 08	2.16	0.02	D+
542.264	60		184 412.0	4d43	5p73	542.2639	0.0015	1.15E + 09	1.30	0.08	D+
544.117	10		183 784.0	4d31	5p63			2.25E + 08	2.00	0.09	D+
546.182	80		183 089.2	4d37	5p55			1.27E + 09	1.24	0.10	D+
546.508	50	p, x	182 979 .9	4d11	5p21			1.59E + 09	1.15	0.19	D+
556.729	80		179 620.6	4d53	5p73	556.7295	0.0013	5.98E + 08	1.55	0.07	D+
559.569	200		178 709.0	4d15	5p17			1.54E + 09	1.14	0.55	D+
560.428	2	x	178 435.1	4d23	5p45	560.4292	0.0018	2.26E + 08	1.97	0.14	D+
560.769	300		178 326.5	4d17	5p17			9.64E + 09	0.34	0.71	C

Table 1. (Continued.)

λ_{obs}(Å)	Intensity		σ_{obs}(cm^{-1})	Even level[a]	Odd level[a]	λ_{Ritz}(Å)	Unc(λ_{Ritz}-Å)	$g_U A$(s^{-1})	log ($g_L f$)	|CF|	Acc.
561.601	10	x	178 062.4	4d21	5p41			1.88E + 08	2.05	0.03	D+
562.444	300		177 795.5	4d17	5p25			4.34E + 09	0.69	0.33	C
564.537	200		177 136.3	4d35	5p63	564.5382	0.0015	1.19E + 09	1.25	0.16	D+
565.300	5	x	176 897.2	4d33	5p45			6.70E + 07	2.49	0.10	D+
566.546	20	ℓ	176 508.2	4d37	5p27			1.65E + 08	2.10	0.03	D+
566.670	300	p	176 469.6	4d45	5p55	566.6725	0.0013	5.13E + 09	0.61	0.34	C
566.819	300		176 423.2	4d53	5p63	566.8261	0.0014	2.37E + 09	0.94	0.18	D+
567.620	80	h	176 174.2	4d21	5p43			4.59E + 08	1.65	0.14	D+
568.284	2000		175 968.4	4p61	p5 1			1.19E + 09	1.24	0.05	D+
569.281	300		175 660.2	4d13	5p11			2.08E + 09	1.00	0.27	D+
573.360	300		174 410.5	4d27	5p35			5.60E + 09	0.56	0.17	C
575.179	500		173 858.9	4d11	5p11			3.29E + 09	0.79	0.58	D+
576.090	10		173 584.0	4d23	5p53	576.0923	0.0019	5.03E + 07	2.60	0.01	E
577.233	20		173 240.3	4d37	5p45			2.04E + 09	0.99	0.09	D+
577.863	500		173 051.4	4d15	5p15			1.10E + 10	0.26	0.69	C
578.737	100		172 790.1	4d31	5p53			9.14E + 08	1.34	0.18	D+
578.811	80		172 768.0	4d45	5p63	578.8171	0.0014	8.03E + 08	1.40	0.05	D+
579.142	400	ℓ	172 669.2	4d17	5p15			1.47E + 10	0.13	0.43	C
579.913	200		172 439.7	4d55	5p55	579.9174	0.0018	1.38E + 09	1.15	0.22	D+
580.321	300	ℓ	172 318.4	4d15	5p13			7.13E + 09	0.45	0.36	C
581.236	200		172 047.2	4d33	5p53			1.44E + 09	1.14	0.26	D+
581.480	300		171 975.0	4d13	5p15			2.49E + 09	0.90	0.66	D+
581.610	200		171 936.5	4d55	5p73	581.6144	0.0018	1.34E + 09	1.16	0.18	D+
583.063	200		171 508 .1	4d33	5p41			1.59E + 09	1.09	0.33	D+
583.970	400		171 241.7	4d13	5p13			7.86E + 09	0.40	0.68	C
584.111	150		171 200.3	4d21	5p33			9.04E + 08	1.33	0.34	D+
584.251	250		171 159.3	4d23	5p43	584.2568	0.0020	1.67E + 09	1.07	0.25	D+
584.517	200	x	171 081.4	4d25	5p43			9.33E + 08	1.32	0.27	D+
586.229	100		170 581.8	4d21	5p31			8.86E + 08	1.34	0.26	D+
588.625	200		169 887.4	4d45	5p27	588.6235	0.0015	1.42E + 09	1.13	0.36	D+
589.367	5	x	169 673.6	4d43	5p41	589.3639	0.0019	1.98E + 08	1.99	0.03	D+
(590.182)		A	(169 439.3)	4d11	5p13			2.20E + 09	0.94	0.71	D+
591.079	100		169 182.1	4d25	5p35			2.29E + 09	0.92	0.35	D+
593.405	200		168 519.0	4d21	5p21			3.21E + 09	0.77	0.66	D+
595.987	5	x	167 788.9	4d43	5p43	595.9900	0.0019	4.71E + 08	1.60	0.07	D+
596.236	5		167 718.8	4d33	5p35			3.91E + 08	1.68	0.12	D+
598.686	400		167 032.5	4d47	5p27			3.31E + 09	0.75	0.65	D+
600.282	1000		166 588.4	4d29	5p27			3.30E + 10	0.25	0.73	C
601.759	2		166 179.5	4d23	5p33			1.23E + 09	1.18	0.15	D+
601.914	50		166 136.7	4d35	5p53	601.9125	0.0017	3.33E + 09	0.74	0.21	C
602.040	100		166 101.9	4d25	5p33			7.35E + 09	0.40	0.59	C
602.387	2000		166 006.2	4d19	5p17			3.36E + 10	0.26	0.80	C
602.932	5		165 856.2	4d55	5p27			5.55E + 08	1.52	0.46	D+
604.002	100		165 562.4	4d23	5p31			4.62E + 09	0.60	0.44	C
604.515	50		165 421.9	4d53	5p53	604.5140	0.0016	1.93E + 09	0.97	0.29	D+
606.493	50		164 882.4	4d53	5p41	606.4912	0.0016	4.18E + 09	0.64	0.71	C
607.378	100		164 642.1	4d33	5p33			2.27E + 09	0.90	0.28	D+
609.525	100	p	164 062.2	4d37	5p35			1.82E + 10	0.01	0.78	C
609.552	90	u	164 054.9	4d25	5p23			7.55E + 09	0.38	0.76	C
610.639	500		163 762.9	4d47	5p45			2.09E + 10	0.07	0.65	C
610.834	1000		163 710.6	4d35	5p43	610.8309	0.0018	6.00E + 09	0.48	0.36	C
611.614	10		163 501.8	4d23	5p21			2.05E + 09	0.94	0.22	D+
612.145	200		163 360.0	4d63	5p61			5.37E + 09	0.52	0.48	C
612.234	50		163 336.2	4d31	5p23			1.49E + 09	1.07	0.40	D+
614.207	5		162 811.6	4d43	5p33	614.2076	0.0020	1.51E + 09	1.07	0.18	D+
615.047	200		162 589.2	4d55	5p45	615.0504	0.0020	2.12E + 09	0.92	0.40	D+
616.547	100		162 193.6	4d43	5p31	616.5475	0.0020	2.95E + 09	0.77	0.41	D+
617.422	200		161 963.8	4d33	5p21			2.16E + 09	0.91	0.29	D+

Table 1. (Continued.)

λ_{obs}(Å)	Intensity		σ_{obs}(cm^{-1})	Even level[a]	Odd level[a]	λ_{Ritz}(Å)	Unc(λ_{Ritz}-Å)	$g_U A$(s^{-1})	log $(g_L f)$	|CF|	Acc.
617.999	5		161 812.6	4d35	5p35	617.9987	0.0019	2.77E + 08	1.80	0.06	D+
618.172	200		161 767.3	4d45	5p53	618.1718	0.0016	2.80E + 09	0.80	0.25	D+
619.181	50		161 503.7	4d27	5p17			1.22E + 09	1.15	0.23	D+
620.741	2		161 097.8	4d53	5p35	620.7415	0.0017	1.53E + 08	2.05	0.05	D+
621.223	800		160 972.8	4d27	5p25			1.55E + 10	0.05	0.80	C
622.037	100		160 762.1	4d43	5p23	622.0372	0.0020	3.26E + 09	0.72	0.42	C
627.081	200		159 469.0	4d65	5p73	627.0812	0.0019	6.98E + 09	0.38	0.57	C
627.358	10		159 398.6	4d21	5p11			4.46E + 08	1.58	0.09	D+
627.583	50		159 341.5	4d45	5p43	627.5823	0.0017	2.84E + 09	0.78	0.18	D+
627.667	100		159 320.1	4d75	5p83			1.54E + 10	0.04	0.68	C
629.982	20		158 734.7	4d35	5p33	629.9817	0.0019	1.61E + 09	1.02	0.33	D+
632.835	5		158 019.1	4d53	5p33	632.8321	0.0017	8.15E + 08	1.31	0.11	D+
633.968	200		157 736.7	4d55	5p53			7.53E + 09	0.34	0.68	C
635.151	50		157 442.9	4d45	5p35	635.1510	0.0017	1.27E + 09	1.12	0.24	D+
635.318	5		157 401.5	4d53	5p31	635.3164	0.0018	4.21E + 08	1.59	0.10	D+
638.222	5		156 685.3	4d35	5p23	638.2213	0.0020	1.29E + 09	1.10	0.14	D+
639.920	200		156 269.5	4d65	5p63	639.9202	0.0019	4.09E + 09	0.60	0.63	C
640.764	500		156 063.7	4d57	5p55			1.65E + 10	0.01	0.85	D
641.147	5		155 970.5	4d53	5p23	641.1470	0.0018	4.45E + 08	1.56	0.07	D+
641.661	500		155 845.5	4d27	5p15			3.05E + 09	0.73	0.26	C
642.080	40		155 743.8	4d25	5p25			8.32E + 08	1.29	0.48	D+
643.746	50		155 340.8	4d53	5p21	643.7469	0.0019	1.13E + 09	1.15	0.20	D+
643.869	400		155 311.1	4d55	5p43			4.62E + 09	0.54	0.50	C
645.249	2		154 978.9	4d21	5p13			3.77E + 08	1.62	0.17	D+
646.881	2		154 587.9	4d47	5p35			6.90E + 08	1.37	0.13	D+
647.745	100	p	154 381.7	4d23	5p11			1.52E + 09	1.02	0.38	D+
647.816	100		154 364.8	4d45	5p33	647.8152	0.0017	2.33E + 09	0.84	0.26	D+
651.100	30		153 586.2	4d31	5p11			9.61E + 08	1.22	0.78	D+
654.264	2		152 843.5	4d33	5p11			1.02E + 09	1.19	0.31	D+
655.940	10		152 453.0	4d43	5p25			2.88E + 08	1.73	0.17	D+
656.533	20		152 315.3	4d45	5p23	656.5312	0.0018	1.52E + 09	1.01	0.15	D+
661.560	4		151 157.9	4d37	5p17			2.67E + 08	1.75	0.08	D+
662.196	100		151 012.7	4d43	5p11			9.46E + 08	1.21	0.15	D+
663.593	5		150 694.8	4d23	5p15			3.43E + 08	1.65	0.23	D+
663.892	100		150 626.9	4d37	5p25			3.94E + 09	0.58	0.18	C
663.935	5	u, x	150 617.2	4d25	5p15			3.00E + 08	1.70	0.12	D+
665.185	1		150 334.1	4d55	5p33			2.80E + 07	2.73	0.01	E
666.124	100		150 122.2	4d65	5p45			3.19E + 09	0.67	0.40	C
666.835	50		149 962.1	4d23	5p13			3.73E + 08	1.61	0.10	D+
667.185	10		149 883.5	4d25	5p13			2.76E + 08	1.74	0.10	D+
668.970	500		149 483.5	4d57	5p27			4.62E + 09	0.51	0.55	C
670.392	700		149 166.5	4d31	5p13			2.13E + 09	0.84	0.47	D+
673.754	50		148 422.1	4d33	5p13			5.75E + 08	1.41	0.11	D+
673.961	100		148 376.5	4d35	5p25			1.96E + 09	0.88	0.52	D+
674.378	5		148 284.8	4d55	5p23			5.80E + 08	1.40	0.08	D+
683.926	3		146 214.6	4d57	5p45			4.04E + 08	1.55	0.07	D+
687.812	50		145 388.6	4d63	5p51			2.24E + 09	0.80	0.63	C
688.367	5		145 271.3	4d65	5p53			7.18E + 08	1.29	0.24	D+
694.411	2		144 006.9	4d45	5p25			1.44E + 08	1.99	0.03	D+
698.082	100	u	143 249.6	4d35	5p15			1.45E + 09	0.98	0.27	D+
700.055	5		142 845.9	4d65	5p43			4.85E + 08	1.45	0.18	D+
701.587	10		142 534.0	4d53	5p15			3.91E + 08	1.54	0.17	D+
701.674	20		142 516.3	4d35	5p13			8.50E + 08	1.20	0.11	D+
705.214	2		141 800.9	4d53	5p13			9.27E + 07	2.16	0.02	D+
708.275	2		141 188.1	4d85	5p83	708.2769	0.0020	6.05E + 08	1.34	0.10	D+
708.456	5		141 152.0	4d47	5p25			5.80E + 08	1.36	0.05	D+
709.488	2		140 946.7	4d65	5p35			2.36E + 08	1.75	0.30	D+
715.604	10		139 742.1	4d63	5p73			9.63E + 08	1.13	0.27	D+

Table 1. (Continued.)

λ_{obs}(Å)	Intensity		σ_{obs}(cm^{-1})	Even level[a]	Odd level[a]	λ_{Ritz}(Å)	Unc(λ_{Ritz}-Å)	$g_U A$(s^{-1})	log $(g_L f)$	|CF|	Acc.
720.052	10		138 878.9	4d45	5p15			4.34E + 08	1.47	0.09	D+
723.873	2		138 145.8	4d45	5p13			1.22E + 08	2.02	0.02	D+
729.724	10		137 038.1	4d57	5p35			5.03E + 08	1.39	0.15	D+
732.372	5		136 542.6	4d63	5p63			7.52E + 08	1.22	0.23	D+
736.276	10		135 818.6	4d65	5p23			7.16E + 08	1.23	0.23	D+
746.246	20		134 004.1	4d75	5p55			1.24E + 09	0.98	0.55	D+
784.259	50		127 508.9	4d65	5p25			3.45E + 08	1.50	0.21	D+
789.090	50	x	126 728.3	4d83	5p83			6.11E + 08	1.24	0.38	D+
792.305	1		126 214.0	6s13	5p13			1.55E + 09	0.84	0.20	C
796.541	10		125 542.8	4d63	5p53			1.14E + 08	1.97	0.29	D+
802.832	1		124 559.1	6s23	5p21			3.50E + 09	0.47	0.90	C
803.010	500		124 531.5	4d83	5p61			2.80E + 09	0.57	0.64	C
803.806	20		124 408.1	5d65	5p13			1.45E + 08	1.85	0.01	D+
803.974	20		124 382.1	4d41	5p73			6.16E + 08	1.22	0.64	D+
805.445	10		124 155.0	4d75	5p45			7.02E + 07	2.16	0.13	D+
808.568	200	D, x	123 675.4	5d65	5p15			9.03E + 07	2.05	0.01	D+
809.056	100		123 600.8	4d57	5p25			3.76E + 08	1.43	0.08	D+
809.255	50		123 570.4	6s33	5p45			9.49E + 09	0.03	0.72	C
810.226	200		123 422.4	6s15	5p15			1.26E + 10	0.09	0.92	C
810.562	1		123 371.2	6s25	5p45			2.76E + 09	0.57	0.98	C
812.226	1	x	123 118.4	4d63	5p43			5.80E + 07	2.24	0.05	D+
820.482	5		121 879.6	6s23	5p33			3.80E + 09	0.42	0.60	C
821.060	10		121 793.8	6s13	5p11			3.04E + 09	0.51	0.47	C
824.069	20		121 349.1	6s11	5p31			3.31E + 09	0.47	0.90	C
825.195	1000	p	121 183.5	4d41	5p63			1.62E + 09	0.78	0.57	C
828.279	1		120 732.3	6s11	5p33			1.61E + 09	0.78	0.45	C
830.886	1000		120 353.5	6s13	5p25			1.03E + 10	0.03	0.75	C
832.618	1000		120 103.1	6s25	5p27			1.53E + 10	0.20	0.98	C
834.044	5000		119 897.8	4d73	5p55	834.0424	0.0018	8.56E + 08	1.05	0.43	E
837.561	2000		119 394.3	4d73	5p73	837.5570	0.0018	1.52E + 09	0.80	0.35	C
841.738	500		118 801.8	6s23	5p35			1.12E + 10	0.07	0.95	C
843.194	1		118 596.7	6s21	5p43			1.65E + 09	0.75	0.35	C
844.072	2		118 473.3	4d57	5p15			9.53E + 07	1.99	0.06	D+
844.754	500	x	118 377.7	4d51	5p51			2.32E + 09	0.61	0.72	C
847.336	500	D, x	118 016.9	5d65	5p17			1.18E + 08	1.90	0.01	E
849.157	500	dc	117 763.9	6s15	5p17			1.50E + 10	0.21	0.96	C
849.157	500	dc	117 763.9	6s31	5p83			6.86E + 09	0.13	0.97	C
851.623	1		117 422.9	6s33	5p63			2.66E + 09	0.54	0.52	C
853.072	2	p, x	117 223.4	6s25	5p63			2.54E + 09	0.56	0.40	C
856.823	2		116 710.2	6s21	5p41			2.72E + 09	0.52	0.80	C
860.618	5000		116 195.6	4d73	5p63	860.6195	0.0018	2.28E + 09	0.60	0.44	C
860.800	5		116 171.0	6s21	5p53			3.66E + 09	0.39	0.75	C
863.029	20		115 871.0	4d85	5p55	863.0271	0.0019	5.95E + 08	1.17	0.18	D+
863.893	50		115 755.1	6s11	5p43			3.78E + 09	0.37	0.94	C
866.786	5000		115 368.7	4d85	5p73	866.7907	0.0019	1.90E + 09	0.66	0.39	C
873.541	2		114 476.6	6s23	5p53			1.88E + 09	0.67	0.49	C
875.480	10		114 223.1	6s33	5p73			4.39E + 09	0.30	0.60	C
877.011	1		114 023.7	6s25	5p73			1.77E + 09	0.69	0.80	C
879.351	1		113 720.2	6s33	5p55			1.99E + 09	0.64	0.80	D
880.897	200		113 520.6	6s25	5p55			7.80E + 09	0.04	0.79	D
887.057	500		112 732.3	4d51	5p73			6.69E + 08	1.11	0.46	D+
891.516	5000		112 168.5	4d85	5p63	891.5150	0.0020	3.05E + 09	0.44	0.63	C
892.506	5		112 044.1	6s13	5p23			3.83E + 09	0.34	0.49	C
914.995	20		109 290.2	4d85	5p27			3.91E + 08	1.30	0.47	D+
921.000	2		108 577.6	6s33	5p51			1.79E + 09	0.64	0.60	C
925.122	1	x	108 093.9	5d35	5p13			5.65E + 08	1.14	0.03	D+
928.000	1		107 758.6	4d41	5p43			1.24E + 08	1.80	0.15	D+
938.478	5000		106 555.5	4d83	5p51			2.04E + 09	0.57	0.49	C

Table 1. (Continued.)

λ_{obs}(Å)	Intensity		σ_{obs}(cm^{-1})	Even level[a]	Odd level[a]	λ_{Ritz}(Å)	Unc(λ_{Ritz}-Å)	$g_U A$(s^{-1})	log $(g_L f)$	|CF|	Acc.
943.213	100		106 020.6	4d85	5p45			3.05E + 08	1.38	0.30	D+
945.016	150		105 818.3	5d41	5p33			2.19E + 09	0.53	0.74	C
(955.500)		A	(104 657.28)	4d73	5p41			1.05E + 09	0.85	0.32	C
972.924	5000	p	102 783.0	4d41	5p33			2.28E + 08	1.49	0.33	D+
973.902	5		102 679.7	5d31	5p11			1.21E + 08	1.76	0.01	D+
983.256	50	x	101 702.9	5d35	5p17			7.73E + 07	1.95	0.04	D+
988.431	5000		101 170.4	4d85	5p53			5.81E + 08	1.07	0.57	D+
990.984	1000		100 909.8	4d83	5p73			4.24E + 08	1.20	0.19	D+
991.356	50		100 871 .9	4d73	5p35			4.03E + 07	2.23	0.14	D+
992.272	2000		100 778.8	5d25	5p13			1.82E + 09	0.57	0.11	C
1009.339	200		99 074.74	5d73	5p45			2.04E + 09	0.51	0.64	C
1012.720	1000		98 743.98	4d85	5p43			4.34E + 08	1.17	0.19	D+
1017.202	500		98 308.89	5d55	5p23			8.45E + 08	0.89	0.03	D
1020.467	1000		97 994.35	4d51	5p41			4.49E + 08	1.17	0.28	D+
1021.266	200		97 917.68	5s21	5p61			7.83E + 07	1.91	0.03	D+
1022.554	200		97 794.35	4d73	5p33			9.17E + 07	1.85	0.05	D+
1023.436	2		97 710.07	4d83	5p63			1.96E + 07	2.51	0.01	D+
1025.821	5000		97 482.89	5d75	5p45			1.07E + 10	0.23	0.73	C
1029.063	500		97 175.78	4d73	5p31			2.53E + 08	1.40	0.35	D+
1030.122	500		97 075.88	5d53	5p33			1.48E + 09	0.63	0.16	C
1032.576	1000		96 845.17	4d85	5p35			4.39E + 08	1.15	0.55	D+
1038.852	5000		96 260.10	5d55	5p33			2.90E + 09	0.33	0.20	C
1040.906	2000		96 070.15	5d27	5p15			3.87E + 09	0.20	0.36	C
1041.006	2000		96 060.93	5d23	5p11			6.16E + 09	0.00	0.60	C
1044.492	2000		95 740.32	5d43	5p21			7.26E + 09	0.08	0.47	C
1050.577	2000		95 185.79	5d11	5p13			6.10E + 09	0.00	0.91	C
1051.358	2000		95 115.08	4d73	5p21			8.84E + 07	1.84	0.09	D+
1052.487	100	D, x	95 013.05	5s13	5p51			5.10E + 07	2.07	0.02	D+
1053.458	500		94 925.47	5d45	5p33			2.32E + 09	0.41	0.24	D
1053.556	2000		94 916.64	5d25	5p25			8.76E + 09	0.16	0.72	C
1055.367	200		94 753.77	5s15	5p55			5.68E + 07	2.02	0.01	D+
1055.966	200	J	94 700.02	5d21	5p11			3.98E + 09	0.17	0.89	C
1059.473	2000		94 386.55	5d25	5p17			1.03E + 08	1.76	0.12	D+
1061.816	1000	dc	94 178.28	5d33	5p21			1.79E + 09	0.52	0.17	C
1061.816	1000	dc, J	94 178.28	5d57	5p27			1.13E + 10	0.28	0.78	C
1064.694	1000		93 923.70	5d35	5p23			4.46E + 09	0.12	0.22	C
1064.821	5000		93 912.50	5d13	5p13			1.28E + 10	0.34	0.88	C
1068.842	2000		93 559.20	5d31	5p21			6.85E + 09	0.07	0.93	C
1068.964	200		93 548.52	5d33	5p23			1.05E + 09	0.75	0.17	C
1072.874	5000		93 207.59	5d15	5p13			1.02E + 10	0.25	0.43	C
1073.192	2000		93 179.97	5d13	5p15			4.58E + 09	0.10	0.88	C
1074.556	1000	p	93 061.69	5d43	5p33			5.19E + 09	0.05	0.55	C
1081.130	1000	dc	92 495.81	5d17	5p15			2.21E + 10	0.59	0.61	C
1081.130	1000	dc	92 495.81	5d47	5p45			3.61E + 10	0.80	0.95	C
1081.395	5000		92 473.15	5d15	5p15			1.65E + 10	0.46	0.90	C
1084.707	500		92 190.79	5d83	5p61			1.48E + 10	0.42	0.94	C
1085.589	2000	p	92 115.89	5d33	5p31			1.32E + 10	0.37	0.92	C
1085.784	90		92 099.35	5d53	5p43			8.62E + 08	0.82	0.15	C
1088.440	2000		91 874.61	5d35	5p33			1.32E + 10	0.37	0.74	C
1088.758	1000		91 847.78	5d45	5p35			5.43E + 09	0.02	0.59	C
1090.297	500		91 718.13	4d85	5p23			3.06E + 08	1.26	0.18	D+
1092.917	500		91 498.26	5d31	5p31			7.50E + 08	0.87	0.14	C
1094.784	500		91 342.22	5s25	5p83			2.89E + 08	1.29	0.30	D+
1095.491	2000		91 283.27	5d55	5p43			1.30E + 10	0.37	0.76	C
1097.314	5		91 131.62	4d51	5p33			2.98E + 07	2.28	0.06	D+
1099.589	5000		90 943.07	5d27	5p25			3.23E + 10	0.77	0.98	C
1100.351	1000		90 880.09	5d31	5p33			9.06E + 08	0.79	0.37	C
1101.745	2000		90 765.10	5d11	5p11			2.82E + 09	0.29	0.49	C

Table 1. (Continued.)

λ_{obs}(Å)	Intensity		σ_{obs}(cm^{-1})	Even level[a]	Odd level[a]	λ_{Ritz}(Å)	Unc(λ_{Ritz}-Å)	$g_U A$(s^{-1})	log $(g_L f)$	|CF|	Acc.
1104.807	200	x	90 513.55	4d51	5p31			5.83E + 07	1.98	0.16	D+
(1108.491)		B	(90 215.17)	5d53	5p41			1.16E + 10	0.34	0.90	C
1111.222	200		89 991.02	5d83	5p83			2.82E + 09	0.28	0.78	C
1111.745	200		89 948.68	5d45	5p43			1.34E + 09	0.60	0.07	D
(1113.735)		E	(89 787.93)	5d65	5p63			1.13E + 10	0.32	0.79	C
1114.480	2000		89 727.94	5d73	5p73			7.73E + 09	0.16	0.70	C
1114.688	10 000	J	89 711.20	5d19	5p17			4.43E + 10	0.92	0.99	C
1115.161	1000		89 673.15	5d53	5p53			1.16E + 09	0.67	0.32	C
1115.532	2000		89 643.33	5d29	5p27			4.44E + 10	0.92	1.00	C
1116.101	1000		89 597.63	5d85	5p83			2.49E + 10	0.67	0.98	C
1117.413	1000		89 492.43	5d13	5p11			1.66E + 09	0.51	0.20	C
1118.689	2000		89 390.35	5d37	5p35			3.49E + 10	0.82	0.99	C
1118.987	500	D, x	89 366.54	5s13	5p73			6.71E + 07	1.90	0.01	D+
1125.394	2000		88 857.77	5d55	5p53			5.54E + 09	0.02	0.36	D+
1126.166	500		88 796.86	5d35	5p35			1.19E + 09	0.65	0.11	C
(1127.231)		G	(88 712.97)	5d51	5p73			2.14E + 09	0.39	0.57	C
(1129.374)		C	(88 544.61)	5d63	5p63			7.98E + 09	0.18	0.62	C
1134.603	2000		88 136.56	5d75	5p73			1.17E + 10	0.35	0.65	C
1135.257	500		88 085.78	5d43	5p43			9.15E + 08	0.75	0.10	C
1141.121	1000		87 633.13	5d75	5p55			3.11E + 09	0.22	0.33	D
1142.544	5000		87 523.98	5d45	5p53			1.45E + 10	0.46	0.73	C
1143.696	1000		87 435.82	4d73	5p25			1.58E + 07	2.51	0.04	D+
1143.930	2000		87 417.94	5d41	5p63			3.49E + 09	0.16	0.57	C
1144.579	5000		87 368.37	5d17	5p25			3.33E + 09	0.18	0.25	C
1150.770	2000		86 898.34	5d35	5p43			7.27E + 09	0.16	0.67	C
1151.571	2000		86 837.89	5d17	5p17			1.13E + 10	0.35	0.99	C
1151.851	1000		86 816.78	5d15	5p17			1.81E + 09	0.45	0.83	C
1154.620	2000		86 608.58	5d25	5p23			1.26E + 10	0.40	0.59	C
1154.902	1000		86 587.43	5d65	5p73			2.10E + 09	0.38	0.21	C
1155.225	1000		86 563.22	4d41	5p13			6.92E + 07	1.86	0.23	D+
1158.574	2000		86 313.00	5d23	5p23			6.05E + 09	0.08	0.76	C
(1161.638)		F	(86 085.32)	5d65	5p55			8.72E + 09	0.24	0.53	D+
1162.848	1000		85 995.76	4d73	5p11			9.04E + 07	1.75	0.08	D+
1164.083	500		85 904.53	5d31	5p43			2.39E + 08	1.32	0.10	D+
1167.411	2000		85 659.63	5d43	5p53			2.74E + 09	0.25	0.39	C
1187.404	50	x	84 217.33	5d41	5p73			1.15E + 09	0.61	0.81	C
(1189.322)		I	(84 081.49)	5d73	5p51			4.76E + 09	0.04	0.74	C
1204.078	150	H, x	83 051.10	5d51	5p51			4.76E + 09	0.00	0.86	C
1314.039	10		76 101.24	5s23	5p63			1.45E + 09	0.43	0.68	C
1330.353	1	x	75 168.02	5s13	5p53			7.65E + 08	0.69	0.18	C
1406.536	10		71 096.65	5s21	5p63			2.55E + 08	1.12	0.65	D+
1411.561	5		70 843.56	5s13	5p35			1.64E + 08	1.31	0.02	D+
1416.418	500		70 600.63	5s15	5p23			4.67E + 08	0.85	0.20	C
1417.866	2000		70 528.53	5s33	5p51			2.39E + 09	0.14	0.84	C
1483.078	500		67 427.34	5s11	5p53			4.13E + 08	0.87	0.27	C
1489.263	100		67147.31	5s13	5p31			2.61E + 08	1.06	0.15	C
1495.035	50		66 888.07	5s11	5p41			1.55E + 08	1.29	0.35	D+
1514.569	50 000		66 025.38	5s25	5p55			5.87E + 09	0.31	0.74	D+
1521.702	10 000		65 715.89	5s13	5p23			2.94E + 09	0.01	0.63	C
1526.201	5000		65 522.17	5s25	5p73			1.39E + 09	0.31	0.84	C
1529.397	5000		65 385.25	5s33	5p55			1.53E + 09	0.27	0.87	D
1536.037	2000		65 102.60	5s23	5p53			1.04E + 09	0.44	0.36	C
1538.423	5000		65 001.63	5s11	5p43			2.19E + 09	0.11	0.91	C
1541.255	10 000		64 882.19	5s33	5p73			3.10E + 09	0.05	0.62	C
1548.859	2000		64 563.66	5s23	5p41			1.73E + 08	1.21	0.12	D+
1591.797	50000		62 822.08	5s15	5p17			8.70E + 09	0.52	0.97	C
1595.481	50		62 677.02	5s23	5p43			2.75E + 08	0.98	0.10	C
1604.549	20 000		62 322.81	5s25	5p63			1.63E + 09	0.20	0.42	C

Table 1. (Continued.)

λ_{obs}(Å)	Intensity		σ_{obs}(cm^{-1})	Even level[a]	Odd level[a]	λ_{Ritz}(Å)	Unc(λ_{Ritz}-Å)	$g_U A$(s^{-1})	log ($g_L f$)	|CF|	Acc.
1605.358	10		62 291.40	5s15	5p25			1.29E + 08	1.30	0.06	D+
1621.198	20 000		61 682.78	5s33	5p63			1.28E + 09	0.30	0.49	C
1621.441	20000		61 673.54	5s31	5p83			3.96E + 09	0.19	0.96	C
1645.331	50 000		60 778.04	5s23	5p35			5.80E + 09	0.37	0.97	C
1663.953	50 000		60 097.85	5s21	5p53			2.02E + 09	0.08	0.93	C
1665.978	20000		60 024.80	5s11	5p33			8.35E + 08	0.46	0.54	C
1679.024	20 000		59 558.41	5s21	5p41			1.35E + 09	0.25	0.94	C
1681.349	10000		59 476.05	5s31	5p61			1.84E + 09	0.11	0.97	C
1682.238	50 000		59 444.62	5s25	5p27			7.47E + 09	0.50	0.98	C
1683.307	20 000		59 406.87	5s11	5p31			1.48E + 09	0.20	0.94	C
1724.855	1000		57 975.89	5s11	5p23			6.61E + 08	0.53	0.36	C
1733.090	50 000		57 700.41	5s23	5p33			1.77E + 09	0.10	0.65	C
1733.928	50000		57 672.52	5s21	5p43			1.09E + 09	0.31	0.65	C
1741.944	100 000		57407.13	5s13	5p25			5.00E + 09	0.36	0.98	C
1749.353	50 000		57 163.99	5s15	5p15			4.87E + 09	0.35	0.96	C
1751.844	50		57 082.71	5s23	5p31			1.76E + 08	1.09	0.16	C
1772.078	50 000		56 430.92	5s15	5p13			2.43E + 09	0.06	0.92	C
1780.139	2000		56 175.39	5s25	5p45			9.92E + 08	0.32	0.95	C
1786.788	20000		55 966.35	5s13	5p11			1.38E + 09	0.19	0.95	C
1800.659	50 000		55 535.22	5s33	5p45			3.62E + 09	0.25	0.78	C
1817.490	5000		55 020.94	5s23	5p21			1.22E + 09	0.22	0.96	C
1940.003	10 000		51 546.31	5s13	5p13			4.54E + 08	0.59	0.35	C
1974.492	3	h	50 645.94	5s21	5p23			2.04E + 08	0.92	0.19	C

[a] Level codes are explained in table 2.
Symbols: dc, doubly classified; p, perturbed; u, unresolved from close line; s, shaded to shorter wavelength; ℓ, shaded to longer wavelength; x, not included in level optimization; h, hazy.
A, not observed due to break in spectrum—Ritz value.
B, greatly perturbed by Si III line—Ritz value.
C, covered by ghost of Si IV line—Ritz value.
D, intensity much higher than expected, not used in level optimization.
E, covered by ghost of Zr V line—Ritz value.
F, covered by Si III line—Ritz value.
G, covered by ghost of Si IV line—Ritz value.
H, uncertain classification, not included in level optimization.
I, covered by neighboring strong lines—Ritz value.
J, even level for this line not included in least-squares fit.

3.3. $4s^24p^45p$ levels

As already mentioned, all levels of this configuration were given in [6]. However, we find that 13 of the 21 levels of this configuration given in [6] were spurious. The following levels from [6] have been replaced by new levels in table 2. (We use here the LS designations from [6], although for this coupling scheme, it is not possible to specify the *J*-value of the core term.):

(1) $(^3P_2)^4P_{3/2}$ at 423 114; now 5p13 at 421 257.96 cm^{-1}
(2) $(^3P_2)^4P_{5/2}$ at 424 592; now 5p15 at 421 991.19 cm^{-1}
(3) $(^3P_1)^2P_{1/2}$ at 436 172; now 5p21 at 434 797.76 cm^{-1}
(4) $(^3P_2)^4D_{3/2}$ at 437 474; now 5p23 at 435 427.69 cm^{-11}
(5) $(^3P_0)^4D_{1/2}$ at 438 427; now 5p31 at 436 859.11 cm^{-1}
(6) $(^3P_2)^2P_{3/2}$ at 440 224; now 5p33 at 437 477.01 cm^{-1}
(7) $(^3P_0)^4S_{3/2}$ at 444 078; now 5p43 at 442 453.66 cm^{-1}
(8) $(^3P_1)^2D_{3/2}$ at 445 849; now 5p53 at 444 879.34 cm^{-1}
(9) $(^3P_1)^2S_{1/2}$ at 447 709; now 5p41 at 444 340.07 cm^{-1}
(10) $(^1D_2)^2F_{7/2}$ at 452 408; now 5p27 at 452 999.87 cm^{-1}
(11) $(^1D_2)^2P_{3/2}$ at 472 926; now 5p73 at 459 077.64 cm^{-1}
(12) $(^1S_0)^2P_{3/2}$ at 483 178; now 5p83 at 484 897.26 cm^{-1}
(13) $(^1S_0)^2P_{1/2}$ at 487 131; now 5p61 at 482 699.28 cm^{-1}

The structure of the $4p^45p$ levels is shown in figure 4. The levels are designated in *jl*-coupling.

3.4. $4s^24p^45d$ and $4s^24p^46s$ levels

The structures of the $4p^45d$ and $4p^46s$ configurations are shown in figure 5. As these configurations lie very close in energy, we treat them together.

A number of $4p^45d$ and $4p^46s$ levels were established by Chaghtai *et al* [5], based on their observation of resonance lines in the 174–200 Å region. They reported almost all of the levels that could make transitions to the ground term, that is levels with $J = 1/2$, $3/2$ or $5/2$. Only $4p^4(^3P)5d$ $^4D_{5/2}$ was missing. These levels were given again in [6], some with improved accuracy. Our present work confirms most of these levels, improves their accuracies, and provides values for the

Table 2. Odd parity energy levels (cm^{-1}) of Zr VI.

Configuration	Term	J	Desig.[a]	Energy	Uncert.	No. trans.[b]
$4s^24p^5$	^2P	3/2	p5 3	0.00	0.80	55
		1/2	p5 1	15 602.78	0.97	32
$4s^24p^45p$	$(^3P_2)[1]$	3/2	5p13	421 257.96	0.12	20
	$(^3P_2)[2]$	5/2	5p15	421 991.19	0.19	17
	$(^3P_2)[1]$	1/2	5p11	425 678.16	0.18	15
	$(^3P_2)[3]$	5/2	5p25	427 118.65	0.14	17
	$(^3P_2)[3]$	7/2	5p17	427 649.11	0.20	13
	$(^3P_1)[0]$	1/2	5p21	434 797.76	0.21	12
	$(^3P_2)[2]$	3/2	5p23	435 427.69	0.15	20
	$(^3P_0)[1]$	1/2	5p31	436 859.11	0.16	13
	$(^3P_1)[2]$	3/2	5p33	437 477.01	0.13	26
	$(^3P_1)[2]$	5/2	5p35	440 554.88	0.17	20
	$(^3P_0)[1]$	3/2	5p43	442 453.66	0.15	24
	$(^3P_1)[1]$	1/2	5p41	444 340.07	0.17	10
	$(^3P_1)[1]$	3/2	5p53	444 879.34	0.13	20
	$(^1D_2)[3]$	5/2	5p45	449 730.72	0.12	16
	$(^1D_2)[3]$	7/2	5p27	452 999.87	0.21	11
	$(^1D_2)[1]$	3/2	5p63	455 878.16	0.12	19
	$(^1D_2)[2]$	3/2	5p73	459 077.64	0.15	20
	$(^1D_2)[2]$	5/2	5p55	459 580.77	0.14	15
	$(^1D_2)[1]$	1/2	5p51	464 724.05	0.25	9
	$(^1S_0)[1]$	1/2	5p61	482 699.28	0.36	6
	$(^1S_0)[1]$	3/2	5p83	484 897.26	0.33	9

[a] Designations are given with a short form of the configuration (two places) followed by the ordinal number of the calculated J value for the configuration (one place) and the J value (one place). For example 5p73 indicates the seventh level with $J = 3/2$ for the $4p^45p$ configuration. p5 3 and p5 1 indicate the $J = 3/2$ and 1/2 levels of the $4p^5$ configuration, respectively.
[b] Total number of transitions for each level, including those omitted from the level optimization procedure.

$J = 7/2, 9/2$ levels, which cannot radiate to the ground term. Five of the levels of [5, 6] were found to be spurious, and several J-values were revised. The spurious levels were $4p^4(^3P)5d$ $^4P_{1/2}$, $4p^4(^1S)5d$ $^2D_{3/2}$, $4p^46s$ $(^3P_2)_{5/2}$, $4p^46s$ $(^3P_0)_{1/2}$, and $4p^46s$ $(^1S_0)_{1/2}$ (designations from [6]). We confirm the level $4p^46s(^1D_2)_{5/2}$ given in [5] (573 105 cm^{-1}), but reject the revised value given in [6] (573 135 cm^{-1}). Our present value is 573 101.84 cm^{-1}.

Our results for the $4p^45d$ and $4p^46s$ levels are given in table 3. Although this is a complete set, for some levels only tentative values can be given:

(1) The $4p^45d$ $(^3P_2)[0]_{1/2}$ level (5d21) is established by two lines: 192.182 Å to p5 3 and 1055.966 Å to 5p11. However, the 192.182 Å line is largely obscured by a strong line of O IV and so was given a large uncertainty in the level optimization. The value of $4p^45d$ $(^3P_2)[0]_{1/2}$ is thus based almost entirely on 1055.966 Å, 5d21–5p11. A possible confirming transition predicted at 1008.876 Å, 5d21–5p13, was not observed. This could occur because of our use of a filter to eliminate higher order lines that has low-wavelength cutoff near 1000 Å. The level is thus uncertain and was not included in the LSF.

(2) The $4p^45d$ $(^1D_2)[4]_{7/2}$ level (5d47) is established by a single line, 1081.130 Å, 5d47–5p45. This transition is predicted to be extremely strong, so this is likely correct. However, 1081.130 Å is also classified as 5d17–5p15. We thus consider $4p^45d$ $(^1D_2)[4]_{7/2}$ to be tentative and exclude it from the LSF.

(3) The $4p^45d$ $(^1D_2)[3]_{7/2}$ level (5d57) is established by a single line, 1061.816 Å, 5d57–5p27. This transition is predicted to be strong, so this is likely correct. A possible confirming transition 5d55–5d57 cannot be observed due to the presence of a strong line of Si III. Unfortunately, 1061.816 Å is also classified as 5d33–5p21, which makes our value for 5d57 tentative at best. It was not included in the LSF.

(4) The $4p^45d$ $(^3P_2)[4]_{9/2}$ level (5d19) is established by a single line, 1114.688 Å, 5d19–5p17. This transition is predicted to be strong, so this is likely correct. However, since there are no confirming transitions, we consider the level to be tentative.

(5) The $4p^45d$ $(^1D_2)[4]_{9/2}$ level (5d29) is established by a single line, 1115.532 Å, 5d29–5p27. This transition is predicted to be strong, so this is likely correct. However, since there are no confirming transitions, we consider the level to be tentative.

As can be seen, the lines that establish 5d19 and 5d29, 1114.688 Å and 1115.532 Å, have nearly the same wavelength. The matching of these two lines with the 5d19 and

Table 3. Even parity energy levels (cm^{-1}) of Zr VI.

Configuration	Term	*J*	Desig.	Energy	Note[a]	Uncert.	No. trans.[b]
4s4p^6	^{2}S	1/2	4p61	191 570.67		0.89	8
4s^{2}4p^{4}4d	(^{3}P)^{4}D	5/2	4d15	248 940.11		0.85	6
	(^{3}P)^{4}D	7/2	4d17	249 322.89		0.90	4
	(^{3}P)^{4}D	3/2	4d13	250 017.63		0.79	9
	(^{3}P)^{4}D	1/2	4d11	251818.7		1.3	5
	(^{3}P)^{4}F	9/2	4d19	261 642.9		1.4	1
	(^{3}P)^{4}F	7/2	4d27	266 145.41		0.71	5
	(^{1}D)^{2}P	1/2	4d21	266 278.49		0.73	9
	(^{3}P)^{4}F	3/2	4d23	271 296.05		0.57	13
	(^{3}P)^{4}F	5/2	4d25	271 374.36		0.72	8
	(^{3}P)^{4}P	1/2	4d31	272 091.26		0.73	7
	(^{3}P)^{4}P	3/2	4d33	272 834.44		0.69	10
	(^{1}D)^{2}D	3/2	4d43	274 665.60		0.50	11
	(^{3}P)^{2}F	7/2	4d37	276 491.34		0.69	6
	(^{3}P)^{4}P	5/2	4d35	278 742.23		0.47	10
	(^{1}D)^{2}P	3/2	4d53	279 457.21		0.41	14
	(^{1}D)^{2}D	5/2	4d45	283 112.00		0.39	12
	(^{1}D)^{2}G	7/2	4d47	285 967.09		0.65	4
	(^{1}D)^{2}G	9/2	4d29	286 411.5		1.4	1
	(^{3}P)^{2}F	5/2	4d55	287 142.42		0.52	9
	(^{1}D)^{2}F	5/2	4d65	299 608.66		0.45	9
	(^{1}D)^{2}F	7/2	4d57	303 517.22		0.48	6
	(^{1}S)^{2}D	3/2	4d63	319 336.18		0.60	8
	(^{1}S)^{2}D	5/2	4d75	325 576.82		0.75	4
	(^{1}D)^{2}S	1/2	4d41	334 694.92		0.33	7
	(^{3}P)^{2}P	3/2	4d73	339 682.78		0.21	11
	(^{3}P)^{2}D	5/2	4d85	343 709.55		0.22	11
	(^{3}P)^{2}P	1/2	4d51	346 345.56		0.42	7
	(^{3}P)^{2}D	3/2	4d83	358 168.09		0.32	7
4s^{2}4p^{4}5s	(^{3}P$_2$)[2]	5/2	5s15	364 827.11		0.12	7
	(^{3}P$_2$)[2]	3/2	5s13	369 711.65		0.11	11
	(^{3}P$_0$)[0]	1/2	5s11	377 452.05		0.12	8
	(^{3}P$_1$)[1]	3/2	5s23	379 776.65		0.11	10
	(^{3}P$_1$)[1]	1/2	5s21	384 781.44		0.16	8
	(^{1}D$_2$)[2]	5/2	5s25	393 555.34		0.11	7
	(^{1}D$_2$)[2]	3/2	5s33	394 195.47		0.11	7
	(^{1}S$_0$)[0]	1/2	5s31	423 223.46		0.33	4
4s^{2}4p^{4}5d	(^{3}P$_2$)[2]	5/2	5d15	514 465.31		0.46	3
	(^{3}P$_2$)[3]	7/2	5d17	514 487.01		0.30	3
	(^{3}P$_2$)[2]	3/2	5d13	515 170.73		0.31	4
	(^{3}P$_2$)[1]	1/2	5d11	516 443.48		0.37	2
	(^{3}P$_2$)[4]	9/2	5d19	517 360.31	*	0.45	1
				517 292.44	#	0.45	1
	(^{3}P$_2$)[4]	7/2	5d27	518 061.55		0.35	2
	(^{3}P$_2$)[0]	1/2	5d21	520 378.18	*	0.48	2
	(^{3}P$_2$)[1]	3/2	5d23	521 740.06		0.63	4
	(^{3}P$_2$)[3]	5/2	5d25	522 035.99		0.34	5
	(^{3}P$_1$)[1]	1/2	5d31	528 357.52		0.31	7
	(^{3}P$_0$)[2]	3/2	5d33	528 976.13		0.44	4
	(^{3}P$_0$)[2]	5/2	5d35	529 351.71		0.24	7
	(^{3}P$_1$)[3]	7/2	5d37	529 945.22		0.43	1
	(^{3}P$_1$)[1]	3/2	5d43	530 538.91		0.37	6
	(^{3}P$_1$)[2]	5/2	5d45	532 402.86		0.34	5
	(^{3}P$_1$)[3]	5/2	5d55	533 736.95		0.25	5
	(^{3}P$_1$)[2]	3/2	5d53	534 552.78		0.29	5
	(^{1}D$_2$)[4]	7/2	5d47	542 226.54	*	0.45	1
	(^{1}D$_2$)[4]	9/2	5d29	542 643.20	*	0.45	1
				542 711.07	#	0.45	1
	(^{1}D$_2$)[0]	1/2	5d41	543 295.84		0.41	5

Table 3. (Continued.)

Configuration	Term	J	Desig.	Energy	Note[a]	Uncert.	No. trans.[b]
	$(^1D_2)[1]$	3/2	5d63	544 423		10	2
	$(^1D_2)[2]$	5/2	5d65	545 666.07		0.78	5
	$(^1D_2)[3]$	7/2	5d57	547 178.00	*	0.50	1
	$(^1D_2)[3]$	5/2	5d75	547 213.94		0.28	4
	$(^1D_2)[1]$	1/2	5d51	547 791		11	3
	$(^1D_2)[2]$	3/2	5d73	548 805.54		0.33	4
	$(^1S_0)[2]$	5/2	5d85	574 494.88		0.52	2
	$(^1S_0)[2]$	3/2	5d83	574 889.14		0.74	3
$4s^24p^46s$	$(^3P_2)[2]$	5/2	6s15	545 413.52		0.77	3
	$(^3P_2)[2]$	3/2	6s13	547 471.92		0.42	5
	$(^3P_0)[0]$	1/2	6s11	558 208.73		0.48	4
	$(^3P_1)[1]$	3/2	6s23	559 356.47		0.41	6
	$(^3P_1)[1]$	1/2	6s21	561 050.32		0.41	5
	$(^1D_2)[2]$	5/2	6s25	573 101.84		0.48	6
	$(^1D_2)[2]$	3/2	6s33	573 301.14		0.35	6
	$(^1S_0)[0]$	1/2	6s31	602 661.0		4.0	3

[a] Designations are explained in table 2; 4p61 indicates the $^2S_{1/2}$ level of $4s4p^6$.
[b] Total number of transitions for each level, including those omitted from the level optimization procedure.
Notes:
*Tentative value; not included in least-squares fit.
#Alternate value for interchange of classifications of □1114.688 and 1115.532 Å.

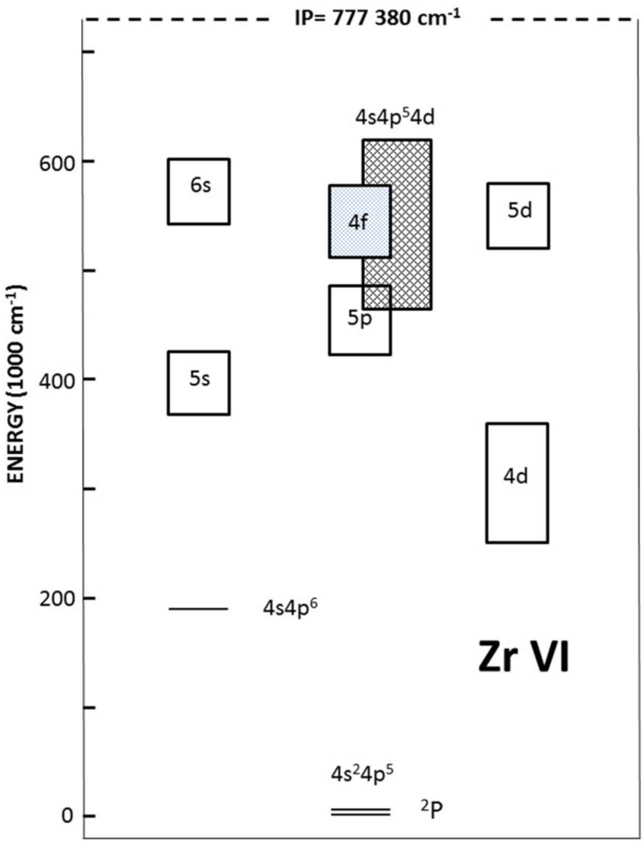

Figure 1. Schematic overview of the configurations of Zr VI. The calculated positions of the $4s^24p^44f$ and $4s4p^54d$ configurations, for which no levels are known, are also shown.

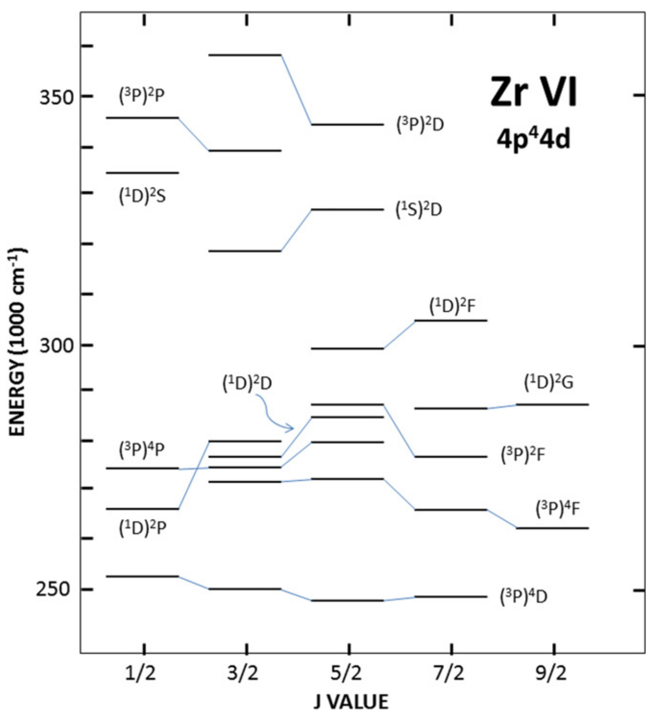

Figure 2. Structure of the $4s^24p^44d$ configurations of Zr VI.

5d29 levels was done so as to produce the best agreement with the LSF predictions. An effort was made to resolve the question by an isoelectronic comparison. However, the lines were again predicted to be so close that a clear resolution was

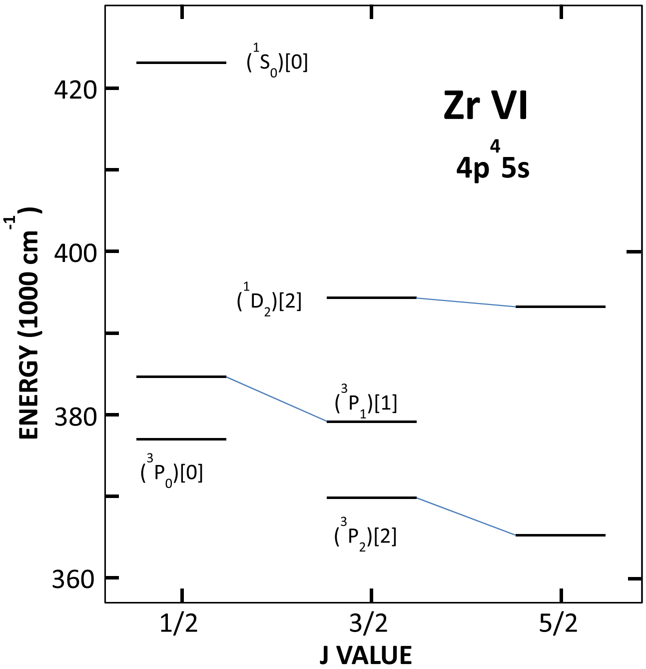

Figure 3. Structure of the $4s^24p^45s$ configurations of Zr VI. The levels are designated in *jl*-coupling.

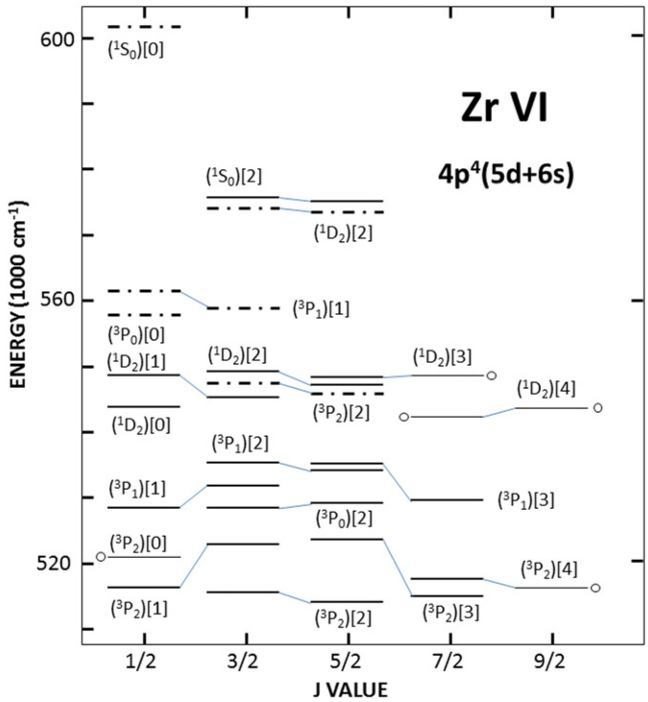

Figure 5. Structures of the $4s^24p^45d$ and $4s^24p^46s$ configurations of Zr VI. The levels are designated in *jl*-coupling. The $4s^24p^46s$ levels are shown as dashed. Levels noted by open circles are tentative.

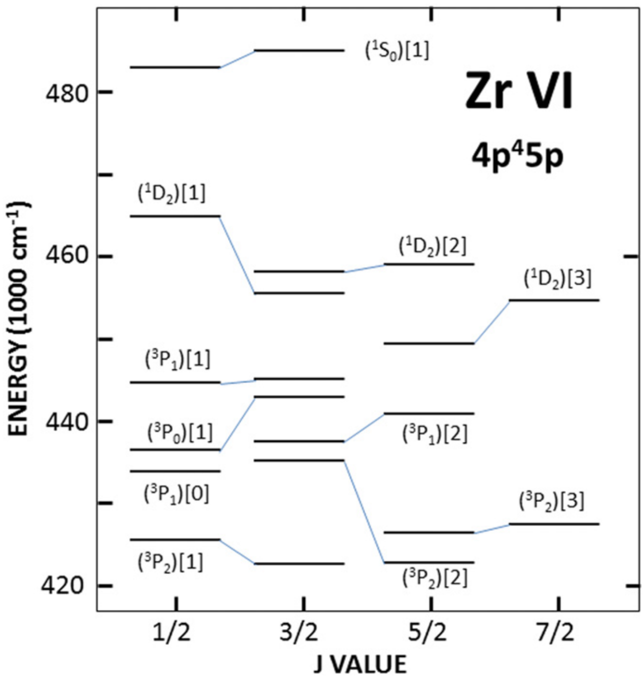

Figure 4. Structure of the $4s^24p^45p$ configuration of Zr VI. The levels are designated in *jl*-coupling.

not possible. In table 3, we list alternative values for the 5d19 and 5d29 levels that would apply if the designations were interchanged.

3.5. Higher $4p^4$nd and $4p^4$ns levels

In [5] some levels of these configurations were located on the basis of resonance lines in the region around 159 Å. In [6] a number of these levels were reported to make transitions to levels of $4p^45p$. In our present observations many of these lines do not appear as belonging to Zr VI, and we thus conclude that the results for these configurations in [5, 6] cannot be accepted without further confirmation.

4. Theoretical Interpretation

4.1. Odd parity configurations

As in [11] 'the observed configurations were interpreted theoretically by making LSFs of the energy parameters to the observed levels with the Cowan suite of codes, RCN (Hartree–Fock), RCG (energy matrix diagonalization), and RCE (least-squares parameter fitting) [12]. The Hartree–Fock code was run in a relativistic mode (HFR) with a correlation term in the potential. Breit energies were not included. For the initial calculations the HFR values were scaled by a factor of 0.85 for the direct electrostatic parameters F^k, the exchange electrostatic parameters G^k, and the configuration interaction (CI) parameters R^k'. The odd configurations $4s^24p^5$, $4s^24p^45p$, $4s^24p^44f$, and $4s4p^54d$ were treated as a single group.

The Hartree–Fock and LSF parameters for the odd configurations are given in table 4. For these calculations, the $4p^45p$ exchange electrostatic parameters, G^0(4p5p) and G^2(4p5p), were linked at their HFR ratio. The LSF/HFR ratio of 0.856 is satisfactory. The CI parameters for the $4s^24p^5$–$4s^24p^45p$ interaction were held fixed at their scaled HFR values. All other CI parameters and parameters for $4s^24p^44f$

Table 4. Hartree–Fock and least-squares fitted parameters (cm^{-1}) for the odd configurations of Zr VI. Mean error of fit 229 cm^{-1}.

Configuration	Parameter	HFR	LSF	Unc.	LSF/HFR
$4s^24p^5$	$E_{av}(4s^24p^5)$	9676	9927	172	
	ζ_{4p}	9986	10481	217	1.049
$4s^24p^45p$	$E_{av}(4s^24p^45p)$	448691	443928	52	0.989
	$F^2(4p4p)$	84030	69669	504	0.829
	$\alpha(4p4p)$		−59[a]		
	ζ_{4p}	10556	10858	133	1.031
	ζ_{5p}	2371	2725	108	1.148
	$F^2(4p5p)$	26016	24044	484	0.924
	$G^0(4p5p)$	5518	4725	62[b]	0.856
	$G^2(4p5p)$	7441	6372	84[b]	0.856
Config. interaction					
$4s^24p^5$–$4s^24p^45p$	$R^0(4p4p, 4p5p)$	2417	2054[c]		0.850
	$R^2(4p4p, 4p5p)$	11574	9837[c]		0.850

[a] Fixed at value from $4p^4$ of Zr VII [15].
[b] Linked in LSF fit.
[c] Fixed at scaled HFR value.

Table 5. Calculated energy levels (cm^{-1}) and percentage compositions for the odd levels of Zr VI.

J	Observed	Calculated	O−C	% jl	Percentage composition (LS-coupling)					
3/2	0	0	0		99%	$4s^24p^5(^1S)^2P$				
1/2	15 603	15 603	0		99%	$4s^24p^5(^1S)^2P$	1%	$4s4p^54d(^1P)^2P$		
3/2	421 258	421 351	−93	40%($^3P_2$)[1]	63%	$4p^45p(^3P)^4P$	9%	$4p^45p(^3P)^4S$	9%	$4p^45p(^1D)^2P$
5/2	421 991	421 956	36	79%($^3P_2$)[2]	68%	$4p^45p(^3P)^4P$	24%	$4p^45p(^3P)^4D$	4%	$4p^45p(^1D)^2D$
1/2	425 678	426 061	−383	54%($^3P_2$)[1]	44%	$4p^45p(^3P)^4P$	24%	$4p^45p(^3P)^2P$	20%	$4p^45p(^1D)^2P$
5/2	427 119	427 158	−40	73%($^3P_2$)[3]	60%	$4p^45p(^3P)^2D$	15%	$4p^45p(^3P)4P$	13%	$4p^45p(^3P)^4D$
7/2	427 649	427 446	203	90%($^3P_2$)[3]	90%	$4p^45p(^3P)^4D$	10%	$4p^45p(^1D)^2F$		
1/2	434 798	434 708	89	55%($^3P_1$)[0]	38%	$4p^45p(^3P)^4P$	27%	$4p^45p(^3P)^4D$	17%	$4p^45p(^3P)^2P$
3/2	435 428	435 079	348	35%($^3P_2$)[2]	33%	$4p^45p(^3P)^4D$	23%	$4p^45p(^3P)^2D$	18%	$4p^45p(^3P)^2P$
1/2	436 859	436 807	52	57%($^3P_0$)[1]	56%	$4p^45p(^3P)^4D$	16%	$4p^45p(^3P)^4P$	15%	$4p^45p(^3P)^2S$
3/2	437 477	437 528	−51	35%($^3P_1$)[2]	49%	$4p^45p(^3P)^4D$	32%	$4p^45p(^3P)^2P$	10%	$4p^45p(^1D)^2P$
5/2	440 555	440408	147	96%($^3P_1$)[2]	60%	$4p^45p(^3P)^4D$	25%	$4p^45p(^3P)^2D$	14%	$4p^45p(^3P)^4P$
3/2	442 454	442 494	−40	67%($^3P_0$)[1]	25%	$4p^45p(^3P)^2D$	25%	$4p^45p(^3P)^4S$	17%	$4p^45p(^3P)^4P$
3/2	444 879	444 863	17	64%($^3P_1$)[1]	44%	$4p^45p(^3P)^2D$	43%	$4p^45p(^3P)^4S$	5%	$4p^45p(^3P)^4P$
1/2	444 340	444 928	−587	63%($^3P_1$)[1]	68%	$4p^45p(^3P)^2S$	13%	$4p^45p(^3P)^2P$	10%	$4p^45p(^3P)^4D$
5/2	449 731	449 565	166	84%($^1D_2$)[3]	84%	$4p^45p(^1D)^2F$	9%	$4p^45p(^3P)^2D$	4%	$4p^45p(^1D)^2D$
7/2	453 000	452 862	138	89%($^1D_2$)[3]	89%	$4p^45p(^1D)^2F$	10%	$4p^45p(^3P)^4D$		
3/2	455 878	455 924	−46	58%($^1D_2$)[1]	58%	$4p^45p(^1D)^2P$	20%	$4p^45p(^1D)^2D$	10%	$4p^45p(^3P)^2P$
3/2	459 078	458 938	139	71%($^1D_2$)[2]	71%	$4p^45p(^1D)^2D$	20%	$4p^45p(^3P)^2P$	8%	$4p^45p(^1D)^2P$
5/2	459 581	459 514	67	90%($^1D_2$)[2]	90%	$4p^45p(^1D)^2D$	4%	$4p^45p(^1D)^2F$	3%	$4p^45p(^3P)^4P$
1/2	464 724	464 776	−52	62%($^1D_2$)[1]	62%	$4p^45p(^1D)^2P$	34%	$4p^45p(^3P)^2P$	2%	$4p^45p(^1S)^2P$
1/2	482 699	482 755	−56	79%($^1S_0$)[1]	79%	$4p^45p(^1S)^2P$	9%	$4p^45P(^3P)^2P$	6%	$4p^45p(^3P)^4D$
3/2	484 897	484 952	−55	81%($^1S_0$)[1]	81%	$4p^45p(^1S)^2P$	4%	$4p^45p(^3P)^2D$	4%	$4p^45p(^3P)^4D$

and $4s4p^54d$ were fixed at their scaled HFR values. The value of the effective interaction parameter $\alpha(4p4p)$ for the $4p^45p$ configuration was fixed at the value observed for the $4p^4$ core of Zr VII [15]. In table 4 only values for the observed configurations $4s^24p^5$ and $4s^24p^45p$ are given.

The calculated level values and eigenvector compositions for the odd configurations are given in table 5. This table gives the percentage compositions for the three leading eigenvector states in LS-coupling and the percentage for the leading eigenvector state in *jl*-coupling. As can be seen there is not much mixing between the $4s^24p^5$ and the $4s^24p^45p$ configurations. Their mutual repulsion is only about 320 cm^{-1}.

4.2. Even parity configurations

The parameters for the even configurations are given in table 6. Here, the $4s4p^6$, $4p^44d$, 5s, 5d, 6s, 6d, and 7s configurations were treated as single group. For the initial calculations the HFR values were scaled by a factor of 0.85 for the direct electrostatic parameters F^k, the exchange electrostatic parameters G^k, and the CI parameters R^k. All the

Table 6. Hartree–Fock and least-squares fitted parameters (cm^{-1}) for the even configurations of Zr VI. Mean error of fit 303 cm^{-1}.

Configuration	Parameter	HF	LSF	Unc.	LSF/HFR
$4s4p^6$	$E_{av}(4s4p^6)$	238 204	225 794	545	0.945
$4s^24p^44d$	$E_{av}(4s^24p^44d)$	291 306	286 394	61	0.982
	$F^2(4p4p)$	82 691	68 538	720	0.829
	$\alpha(4p4p)$		−59[a]		
	ζ_{4p}	10 169	10 463	168	1.029
	ζ_{4d}	719	853	81	1.186
	$F^2(4p4d)$	69 587	60 676	549	0.872
	$G^1(4p4d)$	86 663	69 960	180	0.807
	$G^3(4p4d)$	53 745	45 371	1036	0.844
$4s^24p^45s$	$E_{av}(4s^24p^45s)$	388 500	383 302	110	0.986
	$F^2(4p4p)$	83 691	69 792	1010	0.834
	$\alpha(4p4p)$		−59[a]		
	ζ_{4p}	10 481	10 832	274	1.033
	$G^1(4p5s)$	8701	7486	414	0.860
$4s^24p^45d$	$E_{av}(4s^24p^45d)$	538 379	533 803	70	0.991
	$F^2(4p4p)$	84 085	70 231	594	0.835
	$\alpha(4p4p)$		−59[a]		
	ζ_{4p}	10 550	10 927	141	1.036
	ζ_{5d}	217	274	76	1.265
	$F^2(4p5d)$	19 526	16 999	721	0.871
	$G^1(4p5d)$	10 862	7658[b]	275	0.705
	$G^3(4p5d)$	8028	5660[b]	203	0.705
$4s^24p^46s$	$E_{av}(4s^24p^46s)$	566 615	562 487	112	0.992
	$F^2(4p4p)$	84 157	69 956	914	0.831
	$\alpha(4p4p)$		−59[a]		
	ζ_{4p}	10 581	11 023	237	1.042
	$G^1(4p6s)$	2783	2415	380	0.868
Config. interaction					
$4s4p^6$–$4s^24p^44d$	$R^1(4p4p, 4s4d)$	95 949	74 285[c]	461	0.774
$4s4p^6$–$4s^24p^45d$	$R^1(4p4p, 4s5d)$	32 261	24 977[c]	155	0.774
$4s4p^6$–$4s^24p^45s$	$R^1(4p4p, 4s5s)$	3749	3186[d]		0.850
$4s4p^6$–$4s^24p^46s$	$R^1(4p4p, 4s6s)$	875	744[d]		0.850
$4s^24p^44d$–$4s^24p^45s$	$R^2(4p4d, 4p5s)$	−8467	−7197[d]		0.850
	$R^1(4p4d, 5s4p)$	−1073	−912[d]		0.850
$4s^24p^44d$–$4s^24p^46s$	$R^2(4p4d, 4p6s)$	−5150	−4378[d]		0.850

[a] Fixed at value from $4p^4$ of Zr VII [15].
[b, c] Linked in groups in LSF fit.
[d] Fixed at scaled HFR value.

parameters that were allowed to vary were well defined in the fit and have reasonable ratios to the HFR values. The exchange parameters $G^1(4p5d)$ and $G^3(4p5d)$ were linked at their HFR ratio. The CI parameters for the $4s4p^6$–$4s^24p^44d$ and $4s4p^6$–$4s^24p^45d$ interactions were also linked at their HFR ratio. The fitted values are reasonable. The other CI parameters and those for $4p^46d$ and $4p^47s$ were held fixed at their scaled HFR values. As described in [4] the interaction of $4s4p^6$ $^2S_{1/2}$ with the $4s^24p^4(^1D)4d$ ^2S level is great, with a mutual repulsion of ~33 000 cm^{-1}. On the other hand, interaction between $4s4p^6$ and $4s^24p^45d$ is negligible. The value of the effective interaction parameter $\alpha(4p4p)$ for the $4p^44d$, 5s, 5d, and 6s configurations was again fixed at the value observed for the $4p^4$ core of Zr VII [15]. The calculated level values and eigenvector compositions for the even levels are given in table 7. This table gives the percentage compositions for the three leading eigenvector states in LS-coupling and the percentage for the leading eigenvector state in *jl*-coupling, where appropriate. As can be seen, the purity of the states of the $^4p^44d$ configuration in LS-coupling is low, leading to low leading percentages for many of the levels. In order to avoid duplicate names, we have used the second component for the level observed at 279 457 cm^{-1} to designate the level. Even though the $4p^45d$ and $4p^46s$ configurations are practically coincident, there is not much mixing of states. The percentage compositions for the $4s4p^6$, $4s^24p^44d$, and $4s^24p^45s$ configurations are close to those given in [4].

5. $4s4p^6$–$4s^24p^45p$ transitions

Transitions between the $4s4p^6$ and $4s^24p^45p$ configurations are normally forbidden as two electron jumps. However, because of CI between $4s4p^6$ and $4s^24p^44d$, they can in fact take place. We observe six of them in Zr VI. In lower members of the isoelectronic sequence, these transitions occur

Table 7. Calculated energy levels (cm^{-1}) and percentage compositions for the even levels of Zr VI. Observed levels with asterisk were not included in the least-squares fits.

J	Observed		Calculated	O−C	% *jl*	Percentage composition (LS-coupling)					
1/2	191 571		191 569	2		77%	$4s4p^6(^2S)^2S$	23%	$4p^44d(^1D)^2S$		
5/2	248 940		248 803	137		88%	$4p^44d(^3P)^4D$	3%	$4p^44d(^3P)^4F$	3%	$4p^44d(^3P)^4P$
7/2	249 323		249 305	18		91%	$4p^44d(^3P)^4D$	6%	$4p^44d(^3P)^4F$	2%	$4p^44d(^1D)^2F$
3/2	250 018		249 861	157		86%	$4p^44d(^3P)^4D$	4%	$4p^44d(^3P)^4P$	3%	$4p^44d(^1D)^2D$
1/2	251 819		251 854	−35		85%	$4p^44d(^3P)^4D$	7%	$4p^44d(^1D)^2P$	5%	$4p^44d(^3P)^2P$
9/2	26 1643		261 550	93		90%	$4p^44d(^3P)^4F$	10%	$4p^44d(^1D)^2G$		
7/2	266 145		265 981	164		66%	$4p^44d(^3P)^4F$	17%	$4p^44d(^3P)^2F$	13%	$4p^44d(^1D)^2G$
1/2	266 279		267 364	−1085		44%	$4p^44d(^1D)^2P$	37%	$4p^44d(^3P)^2P$	14%	$4p^44d(^3P)^4D$
3/2	271 296		271 001	295		47%	$4p^44d(^3P)^4F$	16%	$4p^44d(^3P)^4P$	13%	$4p^44d(^1S)^2D$
5/2	271 374		271 025	349		93%	$4p^44d(^3P)^4F$	3%	$4p^44d(^3P)^4D$	2%	$4p^44d(^1S)^2D$
1/2	272 091		272 034	57		91%	$4p^44d(^3P)^4P$	5%	$4p^44d(^3P)^2P$	3%	$4p^44d(^1D)^2P$
3/2	272 834		272 884	−50		38%	$4p^44d(^3P)^4P$	30%	$4p^44d(^3P)^4F$	18%	$4p^44d(^1D)^2P$
3/2	274 666		274 573	93		36%	$4p^44d(^1D)^2D$	21%	$4p^44d(^3P)^2D$	15%	$4p^44d(^3P)^4F$
7/2	276 491		276 813	−322		42%	$4p^44d(^3P)^2F$	25%	$4p^44d(^3P)^4F$	20%	$4p^44d(^1D)^2G$
5/2	278 742		278 634	108		74%	$4p^44d(^3P)^4P$	9%	$4p^44d(^1S)^2D$	7%	$4p^44d(^3P)^2D$
3/2	279 457		279 886	−429		40%	$4p^44d(^3P)^4P$	24%	$4p^44d(^1D)^2P$	22%	$4p^44d(^3P)^2P$
5/2	283 112		282 808	304		41%	$4p^44d(^1D)^2D$	21%	$4p^44d(^3P)^2D$	18%	$4p^44d(^3P)^4P$
7/2	285 967		285 629	338		65%	$4p^44d(^1D)^2G$	24%	$4p^44d(^3P)^2F$	10%	$4p^44d(^1D)^2F$
9/2	286 412		285 935	477		90%	$4p^44d(^1D)^2G$	10%	$4p^44d(^3P)^4F$		
5/2	287 142		287 795	−653		65%	$4p^44d(^3P)^2F$	21%	$4p^44d(^1D)^2F$	9%	$4p^44d(^1D)^2D$
5/2	299 609		299 713	−104		76%	$4p^44d(^1D)^2F$	13%	$4p^44d(^3P)^2F$	9%	$4p^44d(^1D)^2D$
7/2	303 517		303 641	−124		80%	$4p^44d(^1D)^2F$	17%	$4p^44d(^3P)^2F$	2%	$4p^44d(^1D)^2G$
3/2	319 336		319 335	1		63%	$4p^44d(^1S)^2D$	25%	$4p^44d(^1D)^2D$	5%	$4p^44d(^1D)^2P$
5/2	325 577		325 582	−5		73%	$4p^44d(^1S)^2D$	14%	$4p^44d(^1D)^2D$	5%	$4p^44d(^3P)^2F$
1/2	334 695		334 774	−79		69%	$4p^44d(^1D)^2S$	20%	$4s4p^6(^2S)^2S$	5%	$4p^44d(^1D)^2P$
3/2	339 683		339 272	411		50%	$4p^44d(^3P)^2P$	36%	$4p^44d(^1D)^2P$	7%	$4p^44d(^1D)^2D$
5/2	343 710		344 309	−599		64%	$4p^44d(^3P)^2D$	21%	$4p^44d(^1D)^2D$	11%	$4p^44d(^1S)^2D$
1/2	346 346		345 581	764		48%	$4p^44d(^3P)^2P$	41%	$4p^44d(^1D)^2P$	7%	$4p^44d(^1D)^2S$
3/2	358 168		358 453	−285		57%	$4p^44d(^3P)^2D$	19%	$4p^44d(^1S)^2D$	14%	$4p^44d(^1D)^2D$
5/2	364 827		364 804	23	92%$(^3P_2)[2]$	92%	$4p^45s(^3P)^4P$	8%	$4p^45s(^1D)^2D$		
3/2	369 712		369 708	4	82%$(^3P_2)[2]$	51%	$4p^45s(^3P)^2P$	38%	$4p^45s(^3P)^4P$	10%	$4p^45s(^1D)^2D$
1/2	377 452		377 471	−19	63%$(^3P_0)[0]$	90%	$4p^45s(^3P)^4P$	9%	$4p^45s(^1S)^2S$		
3/2	379 777		379 741	36	92%$(^3P_1)[1]$	61%	$4p^45s(^3P)^4P$	37%	$4p^45s(^3P)^2P$	2%	$4p^45s(^1D)^2D$
1/2	384 781		384 780	1	72%$(^3P_1)[1]$	94%	$4p^45s(^3P)^2P$	5%	$4p^45s(^1S)^2S$	1%	$4p^45s(^3P)^4P$
5/2	393 555		393 590	−35	92%$(^1D_2)[2]$	92%	$4p^45s(^1D)^2D$	8%	$4p^45s(^3P)^4P$		
3/2	394 196		394 238	−42	87%$(^1D_2)[2]$	87%	$4p^45s(^1D)^2D$	12%	$4p^45s(^3P)^2P$	1%	$4p^45s(^3P)^4P$
1/2	423 224		423 190	34	85%$(^1S_0)[0]$	85%	$4p^45s(^1S)^2S$	8%	$4p^45s(^3P)^4P$	6%	$4p^45s(^3P)^2P$
5/2	514 465		514 521	−56	55%$(^3P_2)[2]$	70%	$4p^45d(^3P)^4D$	10%	$4p^45d(^3P)^4F$	10%	$4p^45d(^3P)^4P$
7/2	514 487		514 569	−82	91%$(^3P_2)[3]$	73%	$4p^45d(^3P)^4D$	19%	$4p^45d(^3P)^4F$	6%	$4p^45d(^1D)^2F$
3/2	515 171		515 206	−35	61%$(^3P_2)[2]$	59%	$4p^45d(^3P)^4D$	20%	$4p^45d(^3P)^4P$	6%	$4p^45d(^1D)^2D$
1/2	516 444		516 516	−72	77%$(^3P_2)[1]$	43%	$4p^45d(^3P)^4D$	27%	$4p^45d(^3P)^4P$	17%	$4p^45d(^3P)^2P$
9/2	517 360	*	517 149	211	90%$(^3P_2)[4]$	90%	$4p^45d(^3P)^4F$	10%	$4p^45d(^1D)^2G$		
7/2	518 062		517 900	162	87%$(^3P_2)[4]$	65%	$4p^45d(^3P)^2F$	22%	$4p^45d(^3P)^4F$	11%	$4p^45d(^1D)^2G$
1/2	520 378	*	520 366	12	82%$(^3P_2)[0]$	53%	$4p^45d(^3P)^4P$	29%	$4p^45d(^3P)^2P$	11%	$4p^45d(^1D)^2S$
3/2	521 740		521 749	−9	65%$(^3P_2)[1]$	37%	$4p^45d(^3P)^4P$	34%	$4p^45d(^3P)^2D$	13%	$4p^45d(^3P)^2P$
5/2	522 036		521 991	45	54%$(^3P_2)[3]$	40%	$4p^45d(^3P)^2D$	24%	$4p^45d(^3P)^2F$	15%	$4p^45d(^3P)4P$
1/2	528 358		528 514	−156	88%$(^3P_1)[1]$	53%	$4p^45d(^3P)^4D$	30%	$4p^45d(^3P)^2P$	9%	$4p^45d(^3P)^4P$
3/2	528 976		528 938	38	68%$(^3P_0)[2]$	69%	$4p^45d(^3P)^4F$	12%	$4p^45d(^3P)^4D$	11%	$4p^45d(^1S)^2D$
5/2	529 352		529 301	51	52%$(^3P_0)[2]$	59%	$4p^45d(^3P)^4F$	14%	$4p^45d(^3P)^4D$	13%	$4p^45d(^3P)^4P$
7/2	529 945		529 891	54	97%$(^3P_1)[3]$	54%	$4p^45d(^3P)^4F$	23%	$4p^45d(^3P)^2F$	22%	$4p^45d(^3P)^4D$
3/2	530 539		530 479	60	59%$(^3P_1)[1]$	28%	$4p^45d(^3P)^4P$	26%	$4p^45d(^3P)^4D$	19%	$4p^45d(^3P)^2D$
5/2	532 403		532 272	131	97%$(^3P_1)[2]$	52%	$4p^45d(^3P)^4P$	27%	$4p^45d(^3P)^2F$	11%	$4p^45d(^3P)^4F$
5/2	533 737		533 656	81	59%$(^3P_1)[3]$	43%	$4p^45d(^3P)^2D$	42%	$4p^45d(^3P)^2F$	4%	$4p^45d(^1S)^2D$
3/2	534 553		534 777	−224	46%$(^3P_1)[2]$	64%	$4p^45d(^3P)^2P$	17%	$4p^45d(^3P)^2D$	7%	$4p^45d(^1D)^2P$
7/2	542 227	*	542 081	146	88%$(^1D_2)[4]$	88%	$4p^45d(^1D)^2G$	8%	$4p^45d(^3P)^2F$	3%	$4p^45d(^3P)^4F$
9/2	542 643	*	542 576	67	90%$(^1D_2)[4]$	90%	$4p^45d(^1D)^2G$	10%	$4p^45d(^3P)^4F$		
1/2	543 296		543 203	93	79%$(^1D_2)[0]$	79%	$4p^45d(^1D)^2S$	10%	$4p^45d(^3P)^4P$	9%	$4p^45d(^1D)^2P$
3/2	544 423		544 296	127	76%$(^1D_2)[1]$	76%	$4p^45d(^1D)^2P$	7%	$4p^45d(^3P)^4P$	6%	$4p^46s(^3P)^2P$

Table 7. (Continued.)

J	Observed		Calculated	O−C	% jl	Percentage composition (LS-coupling)					
5/2	545 413		545 437	−23	91%($^3P_2$)[2]	91%	$4p^46s(^3P)4P$	9%	$4p^46s(^1D)^2D$		
5/2	545 666		545 709	−43	76%($^1D_2$)[2]	76%	$4p^45d(^1D)^2D$	17%	$4p^45d(^1D)^2F$	2%	$4p^45d(^3P)^4D$
5/2	547 214		547 087	127	73%($^1D_2$)[3]	73%	$4p^45d(^1D)^2F$	15%	$4p^45d(^1D)^2D$	7%	$4p^45d(^3P)^2D$
3/2	547 472		547 461	11	82%($^3P_2$)[2]	63%	$4p^46s(^3P)^2P$	20%	$4p^46s(^3P)^4P$	9%	$4p^46s(^1D)^2D$
7/2	547 178	*	547 229	−51	92%($^1D_2$)[3]	92%	$4p^45d(^1D)^2F$	3%	$4p^45d(^3P)^4D$	2%	$4p^45d(^3P)^2F$
1/2	547 791		547 844	−53	67%($^1D_2$)[1]	67%	$4p^45d(^1D)^2P$	23%	$4p^45d(^3P)^2P$	8%	$4p^45d(^1D)^2S$
3/2	548 806		549 016	−210	78%($^1D_2$)[2]	78%	$4p^45d(^1D)^2D$	18%	$4p^45d(^3P)^2D$	1%	$4p^45d(^1D)^2P$
1/2	558 209		558 212	−3	70%($^3P_0$)[0]	86%	$4p^46s(^3P)^4P$	12%	$4p^46s(^1S)^2S$	2%	$4p^46s(^3P)^2P$
3/2	559 357		559 340	17	99%($^3P_1$)[1]	78%	$4p^46s(^3P)^4P$	22%	$4p^46s(^3P)^2P$		
1/2	561 050		561 077	−27	81%($^3P_1$)[1]	92%	$4p^46s(^3P)^2P$	4%	$4p^46s(^3P)^4P$	3%	$4p^46s(^1S)^2S$
5/2	573 102		573 108	−6	91%($^1D_2$)[2]	91%	$4p^46s(^1D)^2D$	9%	$4p^46s(^3P)^4P$		
3/2	573 301		573 265	36	88%($^1D_2$)[2]	88%	$4p^46s(^1D)^2D$	9%	$4p^46s(^3P)^2P$	2%	$4p^45d(^1S)^2D$
5/2	574 495		574483	12	85%($^1S_0$)[2]	85%	$4p^45d(^1S)^2D$	4%	$4p^45d(^3P)^2F$	3%	$4p^45d(^3P)^4P$
3/2	574 889		574 920	−31	81%($^1S_0$)[2]	81%	$4p^45d(^1S)^2D$	6%	$4p^45d(^3P)^4F$	4%	$4p^45d(^3P)^2D$
1/2	602 660		602 671	−11	85%($^1S_0$)[0]	85%	$4p^46s(^1S)^2S$	9%	$4p^46s(^3P)^4P$	5%	$4p^46s(^3P)^2P$

at wavelengths that are long relative to the resonance lines and serve to improve the accuracy of the excited levels. However, as the separation of configurations with different principal quantum number increases with increasing ionization stage, these transitions move to lower wavelength, and their inclusion does not improve the accuracy of the excited levels. For Zr VI, these transitions fall in the same wavelength region as the $4s^24p^5$–$4s^24p^44d$ resonance transitions, so they have practically no effect on the Ritz values for the resonance lines.

6. Ritz wavelengths

We determined Ritz wavelengths for a number of the lines by differencing the energy level values in tables 2 and 3. The uncertainties of the calculated wavelengths were taken to correspond to the square root of the sum of the squares of the uncertainties of the combining levels. In table 1 we show the Ritz wavelengths and uncertainties for lines likely to be suitable as wavelength standards, that is where the uncertainty of the Ritz wavelength is ±0.0020 Å or less. (This table contains all observed lines together with those with Ritz values.) The Ritz values have uncertainties that vary from ±0.0003 Å to ±0.0020 Å.

7. Oscillator strengths

Table 1 lists the transition probabilities g_UA and log g_Lf for each observed line as calculated with wavefunctions obtained from the fitted energy parameters. Here, f is the oscillator strength, g_U is the statistical weight of the upper level $2J_U + 1$ and g_L is the statistical weight of the lower level $2J_L + 1$. The A-values are compared with recently published *ab initio* values in section 9 below.

Since there are no experimental values for the transition probabilities of Zr VI, it is difficult to estimate the uncertainty of the calculated values. One guide is the cancellation factor. This is the ratio of the calculated transition probability to a value calculated with all parts of the wave function taken as positive [12]. Low cancellation factors generally indicate a larger uncertainty in the calculated values. Indeed, many of the values in table 1 have low cancellation factors. To try to obtain a more quantitative estimate of the uncertainties, we attempted to judge the sensitivity of the values to the parameter values used for the calculation. For this, an alternate calculation was performed with parameters that varied by small amounts from those used for the main calculation. The differences in the results were then used to put the uncertainties on a semi-quantitative basis with code letters, as are often used for this purpose. The letter codes define categories of uncertainties in A-values: C (⩽25%), D + (⩽40%), D (⩾50%), E (>50%).

8. Ionization energy

In [4] an estimated value of $n^*(4p^45s)$ of 3.12 ± 0.02 was used to determine an ionization energy of 773 000 ± 5000 cm^{-1}. In [6] this was revised upward to 776 500 ± 500 cm^{-1} on the basis of a Ritz diagram for the $4p^45s$, 6s, and 7s configurations. (No details of the determination were given.) Since four of the eight levels of $4p^46s$ in [6] have now been found to be spurious, this value must be re-determined.

For our new determination we use the centers-of-gravity of the $4p^45s$ and $4p^46s$ configurations together with an estimated value for the change in effective quantum number $\Delta n^*(4p^46s$–$4p^45s) = n^*(4p^46s)$–$n^*(4p^45s)$. This allows us to find the limit of the $4p^4ns$ series, which is the center-of-gravity of the $4p^4$ configuration of Zr VII.

From the observed levels in table 3, we find the centers-of-gravity of the $4p^45s$ and $4p^46s$ configurations as 383 198.13 and 562 514.9 cm^{-1}, respectively. Our value for $\Delta n^*(4p^46s$–$4p^45s)$ is taken from $\Delta n^*(4p^66s$–$4p^65s)$ for the

Table 8. Comparison of wavelengths λ(Å) and transition probabilities A(s^{-1}) for Zr VI calculated with the MCDF2 method of Singh *et al* [18] and the GRASP3 method of Aggarwal and Keenan [19] with present values. Numerals following level names are index numbers used in [18] and [19]. Blank spaces indicate that line was not observed. Acc. is the accuracy estimate.

Lower level		Upper level		λ[18]	λ[19]	λ(pres.)	A[18]	A[19]	A(pres.)	|CF|	Acc.	Int.(obs)
$4s^24p^5\ ^2P_{3/2}$	1	$4s4p^6\ ^2S_{1/2}$	3	528	494.113	522.000	5.30E + 08	1.0518E + 09	1.31E + 09	0.04	D+	2000
		$4s^24p^44d\ (^3P)^4D_{5/2}$	4	410	392.117	401.701	1.17E + 07	2.0308E + 07	9.49E + 06	0.00	E	80
		$(^3P)^4D_{3/2}$	6	408	390.213	399.967	7.76E + 06	1.1017E + 07	1.22E + 07	0.00	E	80
		$(^3P)^4D_{1/2}$	7	405	387.245	397.112	4.75E + 06	5.6982E + 06	1.40E + 07	0.01	E	30
		$(^1D)^2P_{1/2}$	10	376	359.833	375.546	1.28E + 07	2.1200E + 08	1.49E + 07	0.00	E	30
		$(^3P)^4F_{3/2}$	12	372	359.150	368.600	3.35E + 05	5.1086E + 05	2.13E + 08	0.01	D+	250
		$(^3P)^4F_{5/2}$	11	374	360.799	368.494	1.41E + 08	1.0789E + 07	2.14E + 08	0.61	D+	300
		$(^3P)^4P_{1/2}$	13	368	353.993	367.523	4.67E + 08	5.9759E + 08	8.61E + 08	0.15	D+	300
		$(^3P)^4P_{3/2}$	14	368	353.991	366.522	5.50E + 08	7.0038E + 08	5.27E + 08	0.02	D+	200
		$(^1D)^2D_{3/2}$	15	365	351.232	364.080	3.37E + 08	2.5390E + 08	3.80E + 08	0.01	D+	300
		$(^3P)^4P_{5/2}$	17	360	346.875	358.755	1.60E + 08	1.5603E + 08	2.85E + 08	0.02	D+	300
		$(^1D)^2P_{3/2}$	18	358	344.980	357.837	6.97E + 07	1.7608E + 07	5.52E + 07	0.00	D+	30
		$(^1D)^2D_{5/2}$	19	354	340.992	353.221	3.82E + 08	2.6359E + 08	4.00E + 08	0.01	D+	250
		$(^3P)^2F_{5/2}$	22	348	335.698	348.262	1.96E + 08	3.0306E + 08	1.56E + 08	0.01	D+	200p
		$(^1D)^2F_{5/2}$	23	330	318.897	333.768	3.24E + 08	3.9608E + 08	4.95E + 08	0.10	D+	400
		$(^1S)^2D_{3/2}$	25	306	304.453	313.150	1.68E + 09	4.0018E + 09	3.18E + 09	0.11	D+	300
		$(^1S)^2D_{5/2}$	26	301	300.149	307.148	3.16E + 02	2.1104E + 09	5.26E + 05	0.00	E	30
		$(^1D)^2S_{1/2}$	28	279	280.532	298.779	1.63E + 11	9.7116E + 10	1.41E + 11	0.71	C	300
		$(^3P)^2P_{3/2}$	27	281	283.619	294.395	1.56E + 11	1.2527E + 11	1.46E + 11	0.90	C	500
		$(^3P)^2D_{5/2}$	30	274	277.998	290.949	1.29E + 10	1.6154E + 11	1.75E + 11	0.85	C	500
		$(^3P)^2P_{1/2}$	29	275	273.019	288.730	1.91E + 11	6.3978E + 10	1.38E + 10	0.11	D+	200
		$(^3P)^2D_{3/2}$	31	265	268.277	279.198	7.17E + 09	7.1045E + 09	4.46E + 09	0.05	D+	90p
$4s^24p^5\ ^2P_{1/2}$	2	$4s4p^6\ ^2S_{1/2}$	3	574	534.239	568.284	2.40E + 08	4.7253E + 08	5.97E + 08	0.05	D+	2000
		$4s^24p^44d\ (^3P)^4D_{3/2}$	6	435	414.818		3.21E + 05	1.2890E + 00	2.31E + 06	0.00	E	
		$(^3P)^4D_{1/2}$	7	431	411.465	423.344	4.55E + 06	4.8266E + 06	9.63E + 06	0.00	E	5
		$(^1D)^2P_{1/2}$	10	398	380.653	398.919	6.32E + 07	6.0598E + 07	7.66E + 07	0.00	E	80
		$(^3P)^4F_{3/2}$	12	395	379.890	391.094	3.56E + 07	5.1666E + 07	9.18E + 06	0.00	E	100p
		$(^3P)^4P_{1/2}$	13	390	374.124	389.881	2.37E + 07	2.6970E + 07	7.14E + 07	−0.01	E	100p
		$(^3P)^4P_{3/2}$	14	390	374.122	388.754	1.58E + 07	3.2332E + 06	8.46E + 06	0.00	E	20
		$(^1D)^2D_{3/2}$	15	386	371.042	386.007	3.78E + 08	4.0027E + 08	3.88E + 08	−0.01	D+	250
		$(^1D)^2P_{3/2}$	18	379	364.072	378.992	2.06E + 07	1.1180E + 07	1.51E + 07	0.00	E	80
		$(^1S)^2D_{3/2}$	25	321	319.226	329.242	2.20E + 09	6.9689E + 08	3.28E + 09	-0.06	D+	300
		$(^1D)^2S_{1/2}$	28	291	293.028	313.389	8.16E + 09	3.9101E + 10	1.27E + 10	−0.11	C	300
		$(^3P)^2P_{3/2}$	27	294	296.397	308.569	3.20E + 09	2.5940E + 09	1.16E + 09	0.02	D+	100
		$(^3P)^2P_{1/2}$	29	286	284.840	302.351	1.52E + 11	9.6829E + 10	1.28E + 11	−0.87	C	300
		$(^3P)^2D_{3/2}$	31	276	279.682	291.920	1.80E + 11	1.5364E + 11	1.65E + 11	0.85	C	500p

Table 9. Comparison of level energies $E(\mathrm{cm}^{-1})$ for Zr VI calculated with the MCDF2 method of Singh *et al* [18] and the GRASP3 method of Aggarwal and Keenan [19] with present experimental energies. Index numbers are those used in [18] and [19].

Configuration	Term	J	Index	E[18]	E[19]	E(present)
$4s^24p^5$	^2P	3/2	1	0	0.00	0.00
	^2P	1/2	2	15 132.68	15 200.72	15 602.78
$4s4p^6$	^2S	1/2	3	189 416.50	202 382.92	191 570.67
$4s^24p^44d$	$(^3P)^4D$	5/2	4	243 856.87	255 025.79	248 940.11
	$(^3P)^4D$	7/2	5	243 977.58	255 226.61	249 322.89[a]
	$(^3P)^4D$	3/2	6	245 129.81	256 270.21	250 017.63
	$(^3P)^4D$	1/2	7	247 050.21	258 234.49	251 818.7[a]
	$(^3P)^4F$	9/2	8	257 617.85	268 478.41	261 642.9[a]
	$(^3P)^4F$	7/2	9	262 852.29	273 655.78	266 145.41
	$(^1D)^2P$	1/2	10	266 287.05	277 906.98	266 278.49
	$(^3P^{)4}F$	3/2	12	267 351.49	278 434.81	271 296.05
	$(^3P)^4F$	5/2	11	268 547.62	277 162.97	271 374.36
	$(^3P)^4P$	1/2	13	271 422.72	282 491.78	272 091.26
	$(^3P)^4P$	3/2	14	271 795.83	282 492.88	272 834.44
	$(^1D)^2D$	3/2	15	274 341.72	284 711.75	274 665.60
	$(^3P)^2F$	7/2	16	275 087.93	285 754.25	276 491.34[a]
	$(^3P)^4P$	5/2	17	278 072.77	288 288.07	278 742.23
	$(^1D)^2P$	3/2	18	279 170.13	289 871.57	279 457.21
	$(^1D)^2D$	5/2	19	282 736.58	293 262.43	283 112.00
	$(^1D)^2G$	7/2	20	285 041.05	295 528.49	285 967.09[a]
	$(^1D)^2G$	9/2	21	285 304.42	295 244.28	286 411.5
	$(^3P)^2F$	5/2	22	287 334.54	297 886.73	287 142.42
	$(^1D)^2F$	5/2	23	303 235.39	313 598.83	299 608.66
	$(^1D)^2F$	7/2	24	306 845.73	317 300.25	303 517.22
	$(^1S)^2D$	3/2	25	327 037.28	328 458.27	319 336.18
	$(^1S)^2D$	5/2	26	332 337.56	333 168.17	325 576.82[a]
	$(^1D)^2S$	1/2	28	358 608.52	356 465.26	334 694.92
	$(^3P)^2P$	3/2	27	355 733.42	352 586.07	339 682.78
	$(^3P)^2D$	5/2	30	364 819.62	359 714.56	343 709.55
	$(^3P)^2P$	1/2	29	363 414.99	366 274.62	346 345.56
	$(^3P)^2D$	3/2	31	377 428.37	372 749.08	358 168.09

[a] Level energy revised in present work.

one-electron atom Mo VI [16], 1.0338. We use Cowan's Hartree–Fock code to estimate the change in going from Mo VI to Zr VI. For Mo we calculate $\Delta n^*(4p^66s–4p^65s)$ as 1.0367 and for Zr VI we calculate $\Delta n^*(4p^46s–4p^45s)$ as 1.0341, a difference of 0.0026. We thus estimate $\Delta n^*(4p^46s–4p^45s)$ for Zr VI as $1.0338 - 0.0026 = 1.0312$, with an estimated uncertainty of ±0.0015. This produces a limit of $793\,780 \pm 300\ \mathrm{cm}^{-1}$. The effective quantum numbers for Zr VI are $n^*(5s) = 3.102(1)$ and $n^*(6s) = 4.133(3)$. Correcting for the energy of the center-of-gravity of $4p^4$ in Zr VII, $16\,402\ \mathrm{cm}^{-1}$ [15], we obtain for the ionization energy of Zr VI the value $777\,380 \pm 300\ \mathrm{cm}^{-1}$ (96.38 ± 0.04 eV) [17].

9. Comparison with *ab initio* calculations

Recently, two sets of *ab initio* calculations for the levels and oscillator strengths of Zr VI have appeared. Singh *et al* [18] used a multiconfiguration Dirac–Fock approach to make calculations for transitions within the $n = 4$ complex; $4s^24p^5$, $4s4p^6$, $4s^24p^44d$. Aggarwal and Keenan [19] used the general-purpose relativistic atomic structure package GRASP for calculations within the same complex of $n = 4$ configurations. Both calculations are based on new versions of the Grant atomic structure code, as described in their papers [18, 19]. Froese Fischer [20] has recently discussed the accuracy that might be expected from calculations for complex atoms with GRASP, in particular as applied to the Br-like ion W^{39+}. Aggarwal and Keenan also used the flexible atomic code [21].

A comparison of the results of the *ab initio* calculations [18, 19] for the wavelengths and transition probabilities with our present values is given in table 8. The wavelengths for Aggarwal and Keenan [19] in this table are differences of the GRASP3 energies in their table 4. Overall, the wavelengths obtained by Singh *et al* [18] are in better agreement with our present observed wavelengths than those of Aggarwal *et al* [19]. A notable disagreement for the transition probabilities is for the $4s^24p^5\ ^2P_{3/2}–4s^24p^44d\ (^3P)^4F_{3/2}$ transition (indices 1–12), observed at 368.600 Å. (The indices are sequential numbers used in [18] and [19] in their enumeration of the energy levels.) Both Singh *et al* [18] and Aggarwal and Keenan [19] find an extremely low transition probability. However, we obtain a fairly high A-value, and it is indeed

Table 10. Comparison of present percentages (in bold type) for the $4s4p^6$ and $4s^24p^44d$ configurations with the percentage compositions of Singh *et al* [18] (in parentheses). Level values are in cm^{-1}. Index numbers are those used in [18] and [19]. Where there are no values in parentheses, no percentage was given by Singh *et al* [18].

Index	Singh label	*J*	*E*(obs)[a]	Percentage composition							
3	4s ^2S	1/2	191571	**77**(72)%	4s ^2S	**23**(27)%	$(^1D)^2S$				
4	$(^3P)^4D$	5/2	248940	**88**(90)%	$(^3P)^4D$	**3**%	$(^3P)^4F$	**3**%	$(^3P)^4P$		
5	$(^3P)^4D$	7/2	249323	**91**(93)%	$(^3P)^4D$	**6**%	$(^3P)^4F$	**2**%	$(^1D)^2F$		
6	$(^3P)^4D$	3/2	250018	**86**(88)%	$(^3P)^4D$	**4**%	$(^3P)^4P$	**3**%	$(^1D)^2D$		
7	$(^3P)^4D$	1/2	251819	**85**(89)%	$(^3P)^4D$	**7**%	$(^1D)^2P$	**5**%	$(^3P)^2P$		
8	$(^3P)^4F$	9/2	261643	**90**(92)%	$(^3P)^4F$	**10**%	$(^1D)^2G$				
9	$(^3P)^4F$	7/2	266145	**66**(75)%	$(^3P)^4F$	**17**%	$(^3P)^2F$	**13**%	$(^1D)^2G$		
10	$(^1D)^2P$	1/2	266279	**44**(44)%	$(^1D)^2P$	**37**(39)%	$(^3P)^2P$	**14**%	$(^3P)^4D$		
12	$(^3P)^4F$	3/2	271296	**48**(74)%	$(^3P)^4F$	**16**%	$(^3P)^4P$	**13**%	$(^1S)^2D$		
11	$(^3P)^4F$	5/2	271374	**93**(94)%	$(^3P)^4F$	**3**%	$(^3P)^4D$	**2**%	$(^1S)^2D$		
13	$(^3P)^4P$	1/2	272091	**91**(91)%	$(^3P)^4P$	**5**%	$(^3P)^2P$	**3**%	$(^1D)^2P$		
14	$(^3P)^4P$	3/2	272834	**38**(50)%	$(^3P)^4P$	**30**%	$(^3P)^4F$	**18**(20)%	$(^1D)^2P$		
15	$(^1D)^2D$	3/2	274666	**36**(40)%	$(^1D)^2D$	**21**(24)%	$(^3P)^2D$	**15**%	$(^3P)^4F$		
16	$(^3P)^2F$	7/2	276491	**42**(50)%	$(^3P)^2F$	**25**(17)%	$(^3P)^4F$	**20**(20)%	$(^1D)^2G$		
17	$(^3P)^4P$	5/2	278742	**74**(84)%	$(^3P)^4P$	**9**%	$(^1S)^2D$	**7**%	$(^3P)^2D$		
18	$(^3P)^4P$	3/2	279457[b]	**40**(24)%	$(^3P)^4P$	**24**(36)%	$(^1D)^2P$	**22**(22)%	$(^3P)^2P$		
19	$(^1D)^2D$	5/2	283112	**40**(43)%	$(^1D)^2D$	**21**(23)%	$(^3P)^2D$	**18**%	$(^3P)^4P$		
20	$(^1D)^2G$	7/2	285967	**65**(**69**)%	$(^1D)^2G$	**24**(21)%	$(^3P)^2F$	**10**%	$(^1D)^2F$		
21	$(^1D)^2G$	9/2	286412	**90**(92)%	$(^1D)^2G$	**10**%	$(^3P)^4F$				
22	$(^3P)^2F$	5/2	287142	**65**(64)%	$(^3P)^2F$	**21**(19)%	$(^1D)^2F$	**9**%	$(^1D)^2D$		
23	$(^1D)^2F$	5/2	299609	**77**(79)%	$(^1D)^2F$	**12**%	$(^3P)^2F$	**9**%	$(^1D)^2D$		
24	$(^1D)^2F$	7/2	303517	**80**(81)%	$(^1D)^2F$	**16**(16)%	$(^3P)^2F$	**2**%	$(^1D)^2G$		
25	$(^1S)^2D$	3/2	319336	**63**(66)%	$(^1S)^2D$	**25**(25)%	$(^1D)^2D$	**5**%	$(^1D)^2P$		
26	$(^1S)^2D$	5/2	325577	**73**(74)%	$(^1S)^2D$	**14**%	$(^1D)^2D$	**5**%	$(^3P)^2F$		
28	$(^1D)^2S$	1/2	334695	**69**(42)%	$(^1D)^2S$	**20**%	4s ^2S	**5**(21)%	$(^1D)^2P$	**4**(20)%	$(^3P)^2P$
27	$(^3P)^2P$	3/2	339683	**50**(52)%	$(^3P)^2P$	**36**(40)%	$(^1D)^2P$	**7**%	$(^1D)^2D$		
30	$(^3P)^2D$	5/2	343710	**64**(66)%	$(^3P)^2D$	**21**(22)%	$(^1D)^2D$	**11**%	$(^1S)^2D$		
29	$(^3P)^2P$	1/2	346346	**48**(32)%	$(^3P)^2P$	**41**(27)%	$(^1D)^2P$	**7**(30)%	$(^1D)^2S$		
31	$(^3P)^2D$	3/2	358168	**57**(60)%	$(^3P)^2D$	**19**(17)%	$(^1S)^2D$	**14**(17)%	$(^1D)^2D$		

[a] Present value from table 3.
[b] Label for this level in present work is $4p^44d(^1D)^2P_{3/2}$.

observed as a fairly strong line. This transition is nominally forbidden as an inter-combination line in LS-coupling because of the change of spin. However, although the $4p^44d$ level (271 296 cm^{-1} observed value) has a leading percentage composition in LS coupling of 47% $4p^44d$ $(^3P)^4F_{3/2}$, the full percentage compositions show that it actually has a total doublet character of about 36%. This accounts for our calculated transition probability and observed line strength. Singh *et al* [18] report a composition of 74% $4p^44d$ $(^3P)^4F_{3/2}$ for this level, with no secondary percentage mentioned. Percentage compositions were not reported by Aggarwal and Keenan [19].

A number of other striking differences can be seen in table 8. The values found by all three calculations for the $4s^24p^5$ $^2P_{3/2}$–$4s^24p^44d(^1S)^4D_{5/2}$ transition (indices 1–26) are extremely discrepant. The present value is about in the middle of the two found with GRASP. The values for the $4s^24p^5$ $^2P_{1/2}$–$4s^24p^44d(^3P)^4D_{3/2}$ transition (indices 2–6) also disagree by a large amount. Still, they all predict that this will be a very weak line, and in fact it has not been observed.

Both Singh *et al* [18] and Aggarwal and Keenan [19] compare their calculated level values with the observed values given in the NIST Atomic Spectra Database [22]. Since we have made a number of revisions to the $4p^44d$ levels, a new comparison is called for. This is given in table 9.

The percentage compositions for the states of the $4s4p^6$ and $4s^24p^44d$ configurations obtained in the present work are compared with those obtained in the MCDF calculations of Singh *et al* [18] in table 10. The general agreement is qualitatively reasonable. However, there are some striking differences. For example, as a result of the large $4s4p^6$ $^2S_{1/2}$–$4s^24p^44d$ $(^1D)^2S_{1/2}$ interaction mentioned above, we find that the level designated as $4s4p^6$ $^2S_{1/2}$ (index 3) has an admixture of 23% $4p^44d$ $(^1D)^2S_{1/2}$. Singh *et al* [18] find a similar admixture for this level. Correspondingly, we find the level designated as $4p^44d(^1D)^2S_{1/2}$ (index 28) to have an admixture of 20% $4s4p^6$ $^2S_{1/2}$, as would be generally expected. No such admixture is given by Singh *et al* [18]. Presumably, their $4s4p^6$ $^2S_{1/2}$ percentage calculated for this state is below about 16%, the lowest percentage present in their table 3. Other striking differences can be seen for the levels at 271 296 (index 12), 272 834 (index 14), 279 457 (index 18), and 346 346 (index 29) cm^{-1}. Of course, the calculated oscillator strengths depend largely on the admixtures represented by the percentages.

Acknowledgments

The code letters to represent the uncertainties of the transition probabilities were obtained in calculations by Alexander Kramida. We gratefully acknowledge this contribution as well as other helpful discussions. We thank Gillian Nave and Csilla Szabo for their assistance with the image plate measurements.

References

[1] Paul F W and Rense W A 1939 The spectra of Y V and Zr VI *Phys. Rev.* **56** 1110
[2] Chaghtai M S Z 1969 Energy levels of Zr V, VI, VII, Nb VI, VII, VIII, and Mo VII, VIII, IX *J. Opt. Soc. Am.* **59** 969
[3] Chaghtai M S Z 1970 Term analysis of Zr VI, Nb VII, and Mo VIII *Phys. Scr.* **1** 109
[4] Ekberg J O, Hansen J and Reader J 1972 Analysis of the spectrum of five-times ionized zirconium (Zr VI) *J. Opt. Soc. Am.* **62** 1134
[5] Chaghtai M S Z, Rahimullah K and Ahmad S 1974 Transitions 4p–5d, 6d and 4p–6s, 7s in Zr VI and Nb VII *J. Phys. B: At. Mol. Opt. Phys.* **7** 2121
[6] Khan Z A, Chaghtai M S Z and Rahimullah K 1981 Spectrum of five times ionized zirconium (Zr VI) *Phys. Scr.* **23** 837
[7] Reader J and Acquista H 1979 Spectrum and energy levels of four-times ionized zirconium (Zr V) *J. Opt. Soc. Am.* **69** 239
[8] Reader J, Epstein G L and Ekberg J O 1972 Spectra of Rb II, Sr III, Y IV, Zr V, Nb VI, and Mo VII in the vacuum ultraviolet *J. Opt. Soc. Am.* **62** 273
[9] Nave G, Sansonetti C J, Szabo C I, Curry J J and Smillie D G 2011 Use of phosphor image plates for measuring intensities in vacuum ultraviolet spectra *Rev. Sci. Instrum.* **82** 013107
[10] Reader J, Feldman U and Brown C M 2006 Measurement of wavelengths with phosphor storage image plates on a grazing incidence spectrograph *Appl. Opt.* **45** 7657
[11] Reader J and Tauheed A 2015 Spectrum and energy levels of quadruply-ionized molybdenum, Mo V *J. Phys. B: At. Mol. Opt. Phys.* **48** 144001
[12] Cowan R D 1981 *The Theory of Atomic Structure and Spectra* (Berkeley, CA: University of California Press) and Cowan programs RCN, RCN2, RCG, and RCE
[13] Reader J 1997 Transition arrays in atomic spectroscopy with a commercial spreadsheet program *Comput. Phys.* **11** 190
[14] The program ELCALC was written by L J Radziemski Jr The Research Corporation, Tucson, Arizona 85712, The procedure and definition of level value uncertainties are described by Radziemski L J Jr and Kaufman V 1969 *J. Opt. Soc. Am.* **59** 424
[15] Reader J and Acquista N 1976 $4s^24p^4$–$4s4p^5$ Transitions in Zr VII, Nb VIII, and Mo IX *J. Opt. Soc. Am.* **66** 896
[16] Reader J 2010 Spectrum and energy levels of five-times ionized molybdenum, Mo VI *J. Phys. B: At. Mol. Opt. Phys.* **43** 074024
[17] Conversion of the ionization energy from cm^{-1} to eV was done with the factor 8065.54429(18) given by Mohr P J, Taylor B N and Newell D B 2012 CODATA recommended values of the fundamental physical constants: 2010 *Rev. Mod. Phys.* **84** 1527
[18] Singh A K, Aggarwal S and Mohan M 2013 Level energies, lifetimes and radiative rates in the $4p^44d$ configurations of bromine-like ions *Phys. Scr.* **88** 035301
[19] Aggarwal K M and Keenan F P 2014 Energy levels, radiative rates and lifetimes for transitions in Br-like ions with $38 \leqslant Z \leqslant 42$ *Phys. Scr.* **89** 125404
[20] Froese Fischer C 2014 Evaluation and comparison of configuration interaction calculations for complex atoms *Atoms* **2** 2
[21] Gu M F 2008 The flexible atomic code *Can. J. Phys.* **86** 675
[22] Kramida A, Ralchenko Yu, Reader J and NIST ASD Team 2014 *NIST Atomic Spectra Database* (ver. 5.2), [online] Available: (http://physics.nist.gov/asd) [17 July 2015] National Institute of Standards and Technology, Gaith6ersburg, MD